CHEMICAL AND MASS SPECTRAL STUDIES OF 2,2-DIALKYLGLYCINE DECARBOXYLASE

By

Julie La Rocca-Brigham

RECOMMENDED:

Advisory Committee Chair

Chair, Department of Chemistry & Biochemistry

APPROVED:

Interim Dean, College of Science, Engineering, and Mathematics

Dean of the Graduate School

December 15, 2003

Date

CHEMICAL AND MASS SPECTRAL STUDIES OF 2,2-DIALKYLGLYCINE DECARBOXYLASE

A

THESIS

Presented to the Faculty

of the University of Alaska Fairbanks

in Partial Fulfillment of the Requirements

for the degree of

MASTER OF SCIENCE

By

Julie Ann La Rocca-Brigham, B.S.

Fairbanks, Alaska

December 2003

Abstract

2,2-Dialkylglycine Decarboxylase, DGD, is a decarboxylating transaminase that is dependent on a vitamin B6 cofactor, pyridoxal 5'-phosphate (PLP). DGD catalyzes the decomposition of 2-methylalanine in two steps. DGD was purified by ammonium sulfate precipitation and ion-exchange chromatography. The enzyme was reduced to form a covalent bond between the enzyme and the PLP. Also, α-(Trifluoromethyl) Alanine, a suicide mechanism based inhibitor was reacted with DGD until the enzyme was completely inactivated. The nonmodified DGD and these two modified forms of the enzyme were subjected to enzymatic digestion by trypsin. Finally, all three peptide mixtures were analyzed by LC/MS/MS. The mass spectra confirmed the amino acid sequence as predicted by the nucleotides of the gene, and the covalent attachment of the cofactor to lysine 272.

Table of Contents

Chapter 1-Literature Review

Part I - 2,2-Dialkylglycine Decarboxylase (DGD) Page 1

1.1 Purpose of the Project Page 1

1.2 Introduction to 2,2-Dialkylglycine Decarboxylase (DGD) Page 1

1.3 2-Methylalanine Metabolism by Soil Bacteria Page 3

1.4 Characterization of DGD Page 6

1.5 DGD – Gene Sequence Page 9

1.6 The Crystal Structure of DGD Page 12

1.7 DGD – a Decarboxylating Transaminase or a Transaminating Decarboxylase? Page 16

Part II – Fluorinated Amino Acids Page 18

1.8 Fluorinated Amino Acids as Enzyme Inhibitors Page 18

1.9 Fluorinated Amino Acids and Decarboxylases Page 18

1.10 Fluorinated Amino Acids and Transaminases Page 21

1.11 A Mechanism Based Inhibitor of DGD Page 23

1.12 *R* Isomer of F3AIB, a Better Suicide Inhibitor of DGD than the S Isomer Page 25

Part III – Mass Spectroscopy Page 26

1.13 Mass Spectroscopy of Modified Proteins Page 26

Chapter 2 – Materials and Methods

Part I – Materials Page 31

Part II – Methods Page 32

2.1 DGD Purification Page 32

a. Cell Growth Page 32

b. Protein Assay Page 34

c. Ammonium Sulfate Precipitation and Dialysis Page 35

d. Ion-Exchange Chromatography Page 36

e. Activating Column Page 37

2.2 Reduced DGD Purification Page 39

2.3 Digestion Conditions Page 40

2.4 HPLC Page 42

2.5 LC/MS/MS Page 43

Chapter 3 – Results

3.1 DGD Purification Page 45

a. Cell Growth Page 45

b. Protein Assay Page 45

c. Ammonium Sulfate Precipitation and Dialysis Page 45

d. Ion-Exchange Chromatography Page 46

e. Activating Column Page 48

3.2 Reduced DGD Purification Page 49

3.3 Digestion Conditions Page 50

3.4 HPLC Page 55

3.5 LC/MS/MS Page 57

Chapter 4 – Discussion

4.1 Purpose of the Project Page 61

4.2 Tryptic Digestions Page 61

4.3 HPLC Page 63

4.4 LC/MS/MS Page 64

4.5 Future Experiments Page 66

References Page 67

List of Figures

Figure 1.1 – Reactions of DGD Page 3

Figure 1.2 – Proposed mechanisms of AIB Page 5

Figure 1.3a – Two dimensional representation of the helices and β-sheets in DGD Page 13

Figure 1.3b – Three dimensional representation of the helices and β-sheets in DGD Page 14

Figure 1.4 – Isomers of F3AIB showing the R and the S configuration Page 26

Figure 2.1 – pJKDGD-A2.2 plasmid Page 33

Figure 2.2 – Protein concentration standard curve with BSA Page 35

Figure 3.1a - Graph of ion-exchange chromatography data which shows that the highest amount of protein is in fractions 69-71 Page 47

Figure 3.1b - SDS-PAGE which shows that fractions 69-71 contain the purest DGD Page 47

Figure 3.2 – Spectrum scans of DGD without and with 2-methylalanine showing the loss of PLP and the production of PMP after the addition of 2-methylalanine Page 48

Figure 3.3 – Kinetic assay of combined DGD which shows the loss of pyruvate over time Page 49

Figure 3.4 – SDS-PAGE gel of digested trypsinized DGD which shows that the enzyme is completely digested by the lack of a band that corresponds to DGD Page 50

Figure 3.5 – SDS-PAGE gel of digested trypsinized reduced DGD which shows that the reduced enzyme is completely digested by the lack of a band that corresponds to DGD Page 51

Figure 3.6 – Kinetic assay at the beginning of the inhibition reaction showing a healthy enzyme Page 52

Figure 3.7 – Kinetic assay at time 2.5 h which shows that the enzyme is inactivated Page 53

Figure 3.8 – Kinetic assay at time 5 h which shows that the enzyme is completely inactivated Page 53

Figure 3.9 – SDS-PAGE gel of digested trypsinized inhibited DGD which shows that the inhibited enzyme is almost completely digested by the reduction of the band that corresponds to DGD Page 54

Figure 3.10 – RP-HPLC chromatogram of 0.7 μg of digested DGD where each peak represents a peptide in DGD Page 55

Figure 3.11 - RP-HPLC chromatogram of 0.7 μg of digested DGD (top) and 0.7 μg of inhibited digested DGD (bottom) which shows similarity between the nonmodified and modified DGD Page 56

Figure 3.12 – LC/MS/MS of DGD trypsinized with 20% trypsin showing the MS of the digestion mixture and MS/MS of one peptide Page 57

Figure 3.13 – LC/MS/MS of reduced DGD trypsinized with 20% trypsin showing the MS of the digestion mixture and MS/MS of one peptide Page 58

List of Tables

Table 3.1 – UV spectrophotometer results of the purification of DGD showing the protein concentration after sonication and dialysis Page 46

Table 3.2 – UV spectrophotometer results of the purification of DGD showing the protein concentration after ion-exchange chromatography Page 48

Table 3.3 – Peptides of DGD resulting from trypsin cutting at Lys and Arg Page 59

Acknowledgements

University of Alaska Fairbanks

First and foremost I would like to thank Dr. John Keller, my advisor, for being an outstanding professor. He always had time to answer questions and help me with experiments. Also, he provided encouragement and understanding throughout my time as a graduate student. He is an excellent teacher and a wonderful man.

In addition, I would like to thank Dr. Button and Dr. Drew for their encouragement and their participation on my advisory committee. Also, I would like to thank Dr. Clausen and Dr. Rasley for their help with the HPLC. I would also like to thank the entire Chemistry department especially Dr. Cahill, Sheila, Emily and Marlys for their encouragement and support.

Washington University Dept of Chemistry

I would also like to thanks Dr. Vidavsky for performing the LC/MS/MS experiments, and for providing insight into the data.

Ventana Medical Systems, Inc.

Also, I would like to thank Dr. Karen Gray and Tammy Caldwell for their help with the crystallography section, and Dr. Chris Bieniarz for his expertise in LC/MS/MS.

Personal

Finally, above all I thank my sons (Alexander and Devon), my mother and father (Alice and Samuel La Rocca), and my husband (Cyrano) for their support and encouragement.

Chapter 1 - Literature Review

Part I - 2,2-Dialkylglycine Decarboxylase (DGD)

1.1 Purpose of the Project

The question addressed by this project was: "can we use mass spectroscopy to verify the location of the B6 cofactor, pyridoxal 5'-phosphate (PLP) cofactor and the amino acid sequence of 2,2-dialkylglycine decarboxylase (DGD)"? The approach used to answer this question was to digest unmodified and modified DGD with trypsin. Then, LC/MS/MS was used to compare covalently modified (PLP or trifluoroaminoisobutyrate, F3AIB) enzyme with the unmodified enzyme enabling the identification of the peptide of interaction. Based on the results of the LC/MS/MS, one can determine whether or not the inhibitor binding site is the same as the PLP binding site.

The reason that DGD was utilized in this project is because it is a unique in its ability to decarboxylate and transaminate amino acid substrates. Since, DGD is a well studied enzyme it is useful because the results of the amino acid content found by LC/MS/MS can be compared with the known sequence.

1.2 Introduction to 2,2-Dialkylglycine Decarboxylase (DGD)

The enzyme 2,2-dialkylglycine decarboxylase (DGD), was first isolated from the soil bacterium, *Pseudomonas cepacia*, in 1964.(*1*) DGD is a decarboxylating transaminase that is dependent on a vitamin B6 cofactor, pyridoxal 5'-phosphate (PLP). One of the

normal substrates for DGD is 2-methylalanine. The biological role for DGD is unclear; however, it is known that the substrates for DGD, 2-methylalanine and isovaline, are found in cytotoxic peptides that are produced by soil fungi. These substrates are also found in organic components of carbonaceous meteorites; 2-methylalanine and isovaline have been found in an iridium rich Cretaceous-Tertiary boundary layer which is associated with ancient bolide impacts on earth. This enzyme catalyzes the decomposition reaction of 2-methylalanine in two steps. First, the amino acid forms a covalent aldimine intermediate between the α-amino group of the amino acid and the PLP. Carbon dioxide and a ketone are released upon the transfer of the amino group to the cofactor, PLP, resulting in formation of an enzyme bound pyridoxamine 5'-phosphate (PMP) form of the cofactor. Then, amino transfer from the cofactor to the pyruvate results in the formation of L-alanine and regeneration of the cofactor in the PLP form (Figure 1.1).

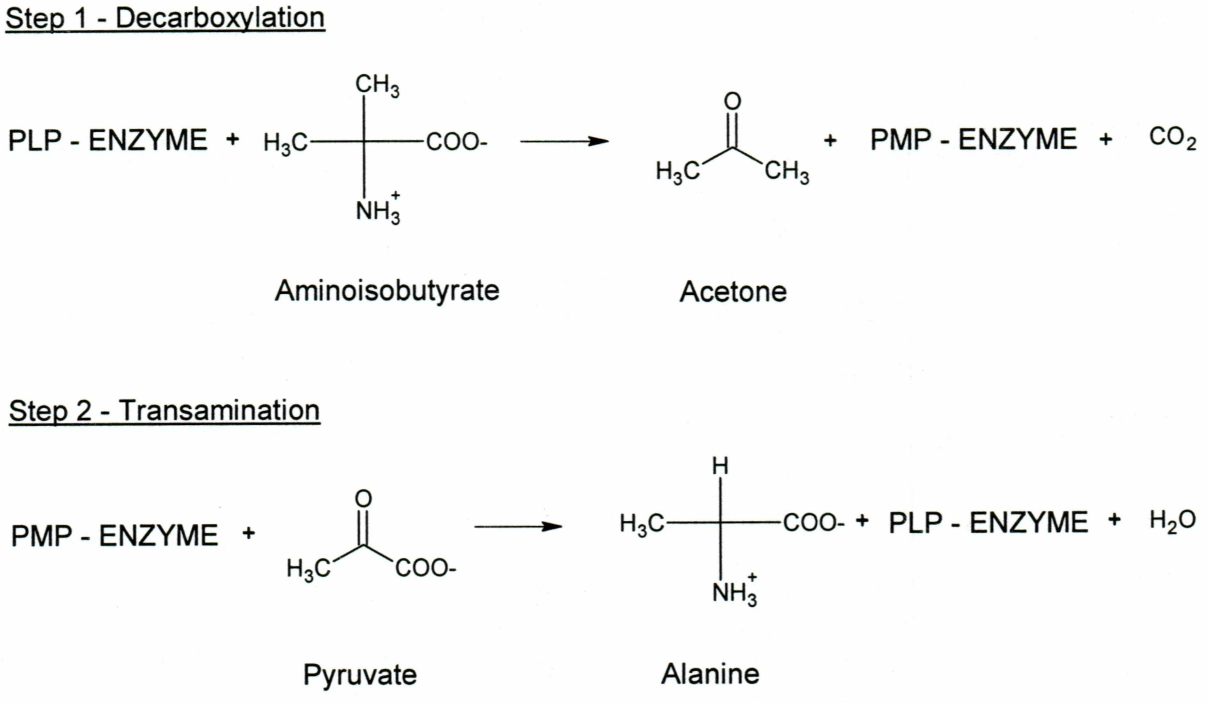

Figure 1.1 – Reactions of DGD.

1.3 2-Methylalanine Metabolism by Soil Bacteria

In 1964, a soil bacterium was found that metabolized 2-methylalanine to form carbon dioxide and acetone.(*2*) The formation of carbon dioxide in the presence of pyruvate was dependent on pyridoxal 5'-phosphate (PLP). To study this phenomenon Aaslestad and Larson grew bacteria on medium containing 2-methylalanine as the sole nitrogen source. They found that this bacterium did grow on the 2-methylalanine with carbon dioxide, acetone and alanine formed as products. Isopropylamine, expected to be the product of normal amino acid decarboxylation, was not found. The optimal pH for the decarboxylation reaction was found to be 7.8, and at this pH 62% of the substrate was

decarboxylated. The authors proposed an enzymatic mechanism for this reaction via the formation of a Schiff base. First, a Schiff base would form between the 2-methylalanine and the cofactor, PLP. Then, the amino acid is decarboxylated and the substrate-cofactor complex is directed to one of two stable Schiff base structures. One structure would form an amine, isopropylamine, and the aldehyde form of the cofactor upon hydrolysis. The other structure would form a keto compound, acetone, and the amine form of the cofactor upon hydrolysis. Since the authors did not detect any free isopropylamine during the metabolism of 2-methylalanine nor did Keller and O'Leary (*3*), the first structure mentioned above seemed unlikely. These experiments support the formation of a keto compound, acetone, and the amine form of the cofactor upon hydrolysis since the formation of acetone was detected.

In 1969, it was shown that soil bacteria that utilize α-aminoisobutyrate (AIB) as a sole nitrogen source can possibly decarboxylate the AIB via two types of decarboxylation reactions (Figure 1.2).(*4*) One type of decarboxylation is direct decarboxylation to form carbon dioxide and isopropylamine. The second is decarboxylation to form carbon dioxide and acetone while transaminating the pyridoxal to pyridoxamine. This type of decarboxylation was termed "decarboxylation-dependent transamination" by Kalyankar and Snell in 1962. Dempsey found that AIB metabolism of bacteria is via the "decarboxylation-dependent transamination" and not via the direct decarboxylation. One reason for this conclusion was that there was a stoichiomeric release of carbon dioxide and acetone from the bacteria. Also, carbon dioxide release from the organism required the presence of pyruvate. For a direct decarboxylation reaction to occur, one enzyme is

required to decarboxylate the AIB and another enzyme would be required to oxidize the amine to convert the nitrogen to a form that can be used by the bacteria. However, only one enzyme is required for the "decarboxylation-dependent transamination". This is because one enzyme converts the AIB to a nitrogen available form of L-alanine. Thus, it was concluded that this enzyme does not decarboxylate by direct decarboxylation. This finding agreed with the conclusion of Aaslestad and Larson in 1964.

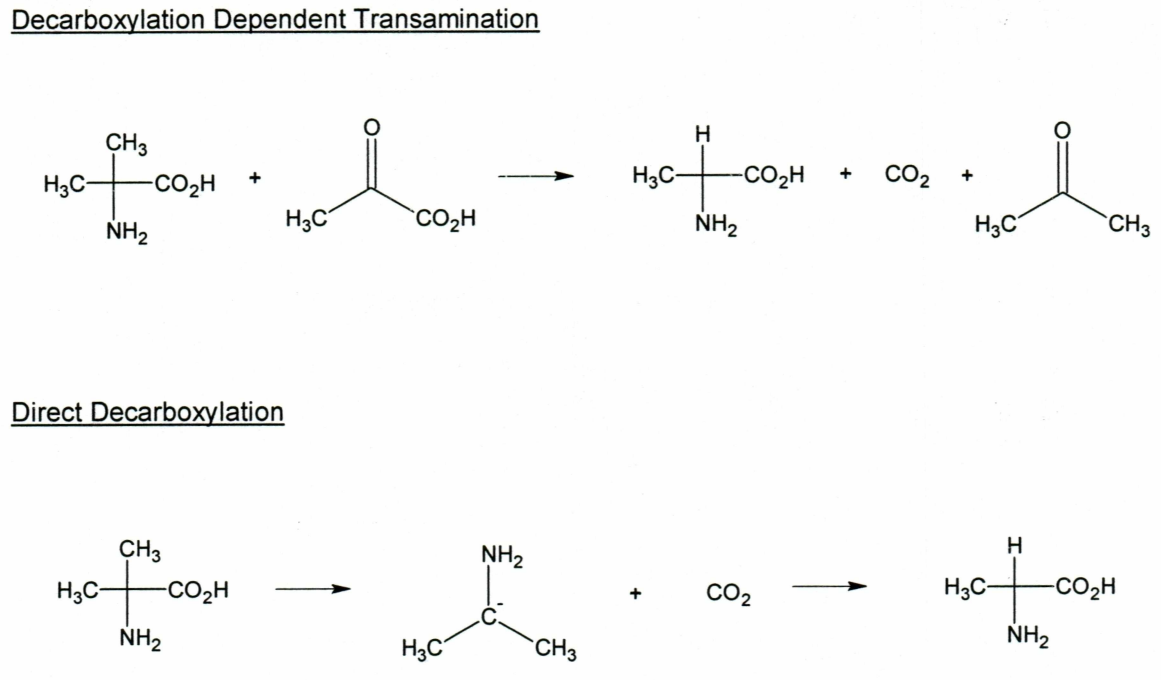

Figure 1.2 – Proposed mechanisms of AIB decarboxylation.

1.4 Characterization of DGD

In 1970, Bailey, Chotamangsa, and Vuttive showed that the mechanism of α-dialkylamino acid transaminase supported the Dunathan hypothesis.(*5, 6*) The Dunathan hypothesis explains how an enzyme uses the rotation of a substrate to control which group bound to an amino acid α-carbon is cleaved. The amino acid bound PLP aldimine is oriented in an activated position so that the bond to be cleaved is perpendicular to the plane of the PLP ring. Dunathan suggested that the orientation could be directed by the binding of the substrate to the α-carboxylate, which is in the active site of the enzyme. An active site residue that is positively charged can form a salt bridge with the carboxylate of the amino acid that is bound to the PLP. If this happens the enzyme can restrict the rotation about the α-carbon to the nitrogen bond thus holding the group to be cleaved in the perpendicular position (*5, 7*). Experiments were performed that analyzed the transamination of D-alanine and L-alanine. When D-alanine was the substrate, decarboxylation occurred prior to transamination. However, when L-alanine was the substrate the hydrogen is located in the position to be cleaved thus no decarboxylation occurs. This implies that amino acids are oriented by binding of the methyl group. Thus, it was concluded that there is a single orientation of the α-dialkylamino acid transaminase active site that leads to the cleavage of the α-carbon otherwise there would have been decarboxylation of the L-alanine.

In 1971, Lamartiniere et al. isolated α-dialkylamino acid transaminase, the enzyme that catalyzes the decarboxylation-dependent transamination metabolism of 2-methylalanine, from *Pseudomonas cepacia* and the molecular weight of this enzyme

was determined to be 47,000 Da.(*8*) They looked among several previously isolated strains of bacteria that showed the enzymatic activity to find a more stable enzyme than the one isolated by Dempsey in 1969. All the bacteria were all grown, harvested, disrupted by sonic oscillation, centrifuged, and purified by ammonium sulfate fractionations. The ammonium sulfate fractions were dialyzed for one week and the fractions were assayed for enzymatic activity. It was shown that the *Pseudomonas cepacia* enzyme retained 78% of its activity over one week, and the specific activity of this enzyme was higher than the specific activity of the enzyme isolated by Dempsey in 1969. It was found that sodium pyruvate is a competitive inhibitor of the PLP form of α-dialkylamino acid transaminase with a K_i of 5 mM. The molecular weight of the enzyme was found to be 188,000 Da by sedimentation equilibrium analysis. An average value of 47,000 Da was found when the sedimentation equilibrium analysis was performed in the presence of 8 M urea and 7 M guanidine HCl. These results suggest that the native enzyme consisted of four subunits thus α-dialkylamino acid transaminase appeared to be a tetramer. However, results obtained from a tryptic map generated by two dimensional chromatography of the tryptic digest of the enzyme suggested that there were eight subunits. There was no explanation for this discrepancy, however, the authors suggested that either the subunits were not completely disassociated or there were errors in the peptide mapping. Electrophoresis of the α-dialkylamino acid transaminase using a polyacrylamide gel containing sodium dodecyl sulfate gave one band. The amino acid composition was determined though analysis with a Beckman 120C amino acid analyzer.

In 1971 Sato, Honma, and Shimomura found that the molecular weight of the AIB decomposing enzyme, isolated from *Pseudomonas sp.*, was 180,000 Da and that it contained four subunits with an individual molecular weight of 45,000 Da.(*9*) The molecular weight of the AIB decomposing enzyme, 180,000 Da, was determined by the Hedrick-Smith method of estimation of molecular weights by disc gel electrophoresis.(*10*) The AIB decomposing enzyme was analyzed via dodecylsulfate-polyacrylamide gel electrophoresis (SDS-PAGE) and a single band at 45,000 Da was found. These results suggested that the AIB decomposing enzyme was a tetramer. The authors also found that analysis by spectrophotometrical titration of the apoenzyme, a protein without its cofactor, at two different concentrations gave an average of four moles of PLP bound per mole of enzyme. This also supports the suggestion that the AIB decomposing enzyme is a tetramer. After analysis of the molecular weight, an inactivation of the AIB decomposing enzyme with phenylglyoxal which reacts with the active site lysine was performed. The phenylglyoxal inactivated the apoenzyme completely; however, the holoenzyme -defined as an enzyme plus its cofactor- was only partially inactivated under the same conditions. Thus, the AIB decomposing enzyme was protected by its cofactor, PLP. It was also found that PLP cannot bind to the phenylglyoxal-inactivated enzyme. The decomposing and transaminating activities were both reduced in parallel with the decrease in PLP binding. These results suggest that the inactivation was caused by the PLP being unable to bind the active site. Also, these results support the idea that there is a single active site for both activities.

1.5 DGD – Gene Sequence

In 1990, the cloning and sequencing of *Pseudomonas cepacia* DNA containing the DGD gene was reported by Keller et al.(*1*) A 4.0-kbp *Pst*I-*Pst*I fragment of the *Pseudomonas cepacia* DNA containing the DGD gene was isolated. First, a *Pst*I restriction digest was performed on the *Pseudomonas cepacia* DNA containing the DGD gene. Then, the fragments were ligated into a plasmid and used to transform *E. coli.* Eventually, the *E. coli* was plated onto agar-2-methylalanine-glucose plates to select for the clone containing the decarboxylase gene. Only *E. coli* clones containing the DGD gene would be able to metabolize 2-methylalanine. After the colonies were grown, a 4.0-kbp fragment was isolated and transferred into pUC19 giving rise to pUC19C7. Also a slightly smaller *Xba*I-*Eco*RI fragment was ligated into pGEM-7Zf(+) which gave rise to pGEM-7Z14. The vector lac promoter is upstream from the DGD gene and the lac promoter points towards the DGD gene. Both of these *E. coli* strains containing pUC19C7 or pGEM-7Z14 grew on 2-methylalanine suggesting that they both contained the functional DGD gene. The + strand of the insert was sequenced from the complementary pGEM-7Z sequences on the left side of the insert, and the - strand of the insert was sequenced from the complementary pUC19 sequences on the right side of the insert. A 3969-nucleotide sequence was determined. The 3' end of the + strand contained the decarboxylase gene and the 3' end of the – strand contained the control gene.

The decarboxylase was purified from *E. coli* JM109 cells containing the plasmid pGEM7Z14/8b, a plasmid containing a truncated derivative of pGEM7Z14.(*1*) The purification of DGD was done in three steps i) ammonium sulfate precipitation ii) ion-exchange chromatography and iii) FPLC ion-exchange chromatography. DGD was then sequenced at the amino terminus by automated Edman degradation. The amino acid sequence, as encoded by the gene, is as follows:

MSLNDDATFWRNARQHLVRYGGTFEPMIIERAKGSFVYDADGRAILDFTSGQMSAVLGHCHPEIV
SVIGEYAGKLDHLFSGMLSRPVVDLATRLANITPPGLDRALLLSTGAESNEAAIRMAKLVTGKYEI
VGFAQSWHGMTGAAASATYSAGRKGVGPAAVGSFAIPAPFTYRPRFERNGAYDYLAELDYAFDL
IDRQSSGNLAAFIAEPILSSGGIIELPDGYMAALKRKCEARGMLLILDEAQTGVGRTGTMFACQRD
GVTPDILTLSKTLGAGLPLAAIVTSAAIEERAHELGYLFYTTHVSDPLPAAVGLRVLDVVQRDGLV
ARANVMGDRLRRGLLDLMERFDCIGDVRGRGLLLGVEIVKDRRTKEPADGLGAKITRECMNLGL
SMNIVQLPGMGGVFRIAPPLTVSEDEIDLGLSLLGQAIERA

The active site peptides are indicated above by the underline. The peptide DGVTPDILTLSK contains the lysine that is thought to bind PLP, lysine 272 (K272).

Next, the active site peptide was sequenced.(*1*) The active site lysine-PLP imine bond was reduced with ^{3}H sodium borohydride. Then, a tryptic digestion was performed and the peptides were separated by reversed phase high performance liquid chromatography (RP-HPLC). The major radioactive peptide was sequenced and all of the peptides matched the wildtype sequence except for K272. Therefore it was concluded that K272 contained the radioactive lysine.

An ATG initiation codon of the 1302-bp DGD structural gene, located at position 1395 of the + strand, was determined to be the start of the only large reading frame that is required for decarboxylase activity. Also, a CCGGAG sequence was found prior to the structural gene. This sequence is similar to the ribosome binding sites of other bacterial genes. The codons used within the decarboxylase coding region are biased towards

codons with G or C in the third position. The amino acid composition was very similar to the amino acid composition determined in 1971 by Lamartiniere et al.(*8*)

Keller et al. stated that the control of the decarboxylase gene is most likely controlled by an upstream repressor.(*1*) To determine the location of the repressor, a series of experiments were carried out. Four *E. coli* strains, all derivations of pGEM-7Z14 with different small amounts of DNA excised from the end of the insert, all showed a repression of decarboxylase activity in the absence of 2-methlyalanine. When 2-methylalanine was provided, all of the plasmids began to express the decarboxylase activity again. Thus, the repressor gene is intact in these four plasmids. However, when the plasmid is truncated by an additional 211-bp (658-bp total) there is loss of control of decarboxylase expression. This deletion removes ten codons from the 3' end of the repressor region; this deletion may or may not delete the entire repressor encoding region. In addition to the above studies, Keller et al. performed other experiments that removed 1314-bp and 1332-bp. This removed some or all of the DNA binding domain. Hence, the remaining plasmid contained a promoter just prior to the decarboxylase gene. This would give RNA polymerase unrestricted access to the DGD promoter thus resulting in constant expression. Expression levels were the same as the 2-methylalanine induced levels that were found with the larger plasmids. These results suggest that the DGD promoter is within 75 nucleotides of the structural decarboxylase gene.

In conclusion, Keller et al. found the sequence for the DGD gene, they showed that the imine bond that PLP forms with the enzyme is via K272, which is in the active site of the enzyme. In addition, they determined the location of the reading frame for the

decarboxylase gene and the repressor gene. Also, an approximate location for the DGD promoter was determined. Now that the DGD gene has been cloned, DGD can be produced more efficiently at large quantities for further experimentation.

1.6 The Crystal Structure of DGD

Toney et al. described the monomeric crystallography of DGD.(*11*) Each monomer contains three major portions: i) a large PLP binding domain, and two smaller domains, ii) a C-terminal domain, and iii) an N-terminal segment (Figure 1.3a and b). The N-terminal segment contains a helix and a three-stranded, antiparallel β-sheet The large PLP binding domain contains seven β-sheets (a, g, f, e, d, b, c), six of which are parallel (Figure 1.3a). This β-sheet cluster is encased by eight α-helices which creates the active site structure. The PLP binding site has been shown to be close to the N-terminus of helix 4 and the C-terminus of strands e and f. The C-terminal domain is characterized by four stranded, antiparallel β-sheet (D, E, F, G), and three α-helices.

The two monomers are tightly associated to form a dimer. Dimerization results in burying of a large solvent accessible surface area, which stabilizes the interaction of both monomers. In fact, the active sites become close enough to each other causing the PLP phosphate atoms to be separated by only 15Å and enabling the sharing of residues from both monomers in the active site domains. This sharing of residues further stabilizes the binding of this critical cofactor, PLP, in the active sites. The dimeric structure is further stabilized at the interface by the formation of a well ordered cluster of charged residues created by helices and loops within the N-termini of both monomers. Helix 2 of each

subunit packs together and forms a hydrophobic region. Thus, the active site consists of amino acids from both monomers which come together to form a well ordered and stable active site. Hydrogen bond interactions between the C-terminus of one strand and the N-terminal β-sheet of an adjacent strand provide a clamp that facilitates one of the closest interactions of both large domains and a small domain of one monomer.

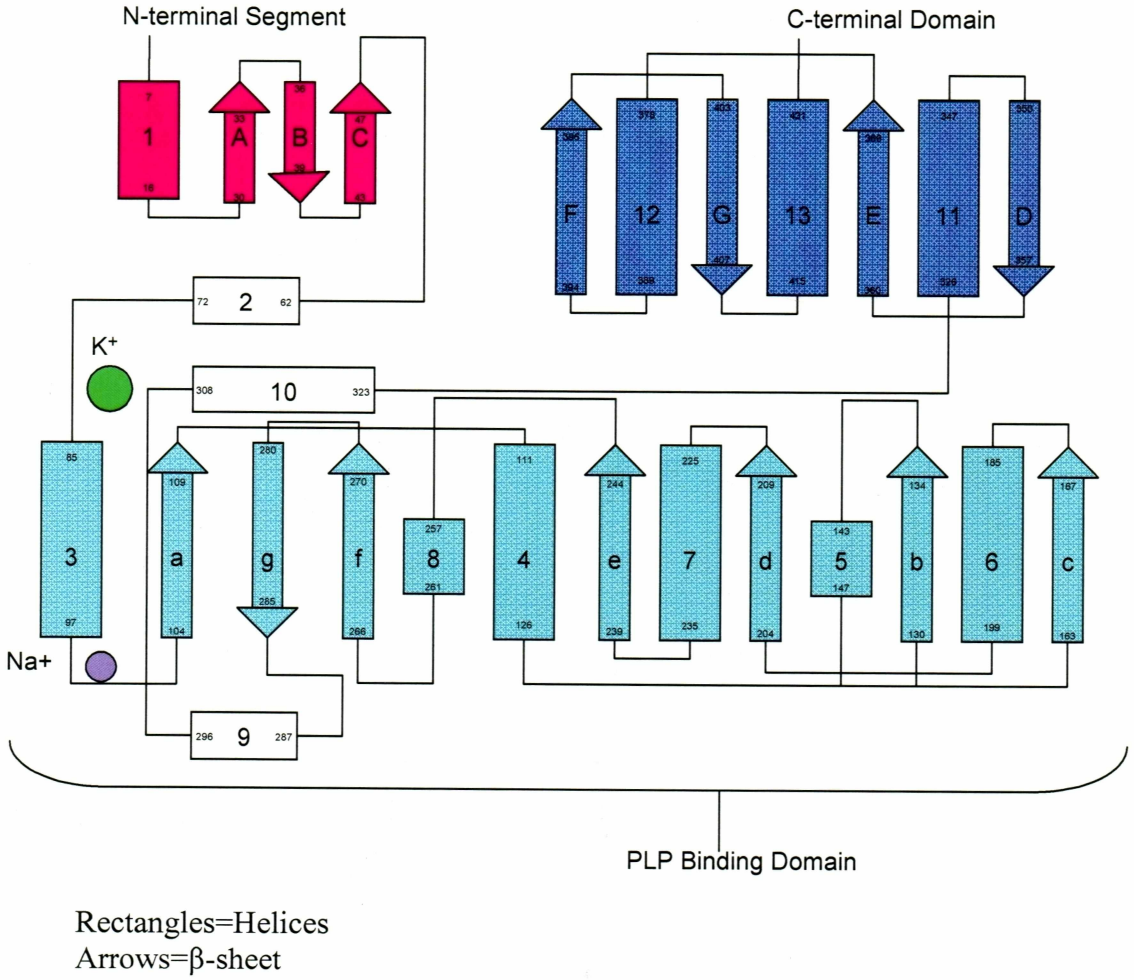

Figure 1.3a – Two dimensional representation of the helices and β-sheets in DGD. Helix 2 is involved in the dimeric interface of DGD. The N-terminal of Helix 4 is near the PLP binding site. Helix 6 is involved in the tetrameric interface. Note: This figure is a reproduction of the original drawing from Toney et al.

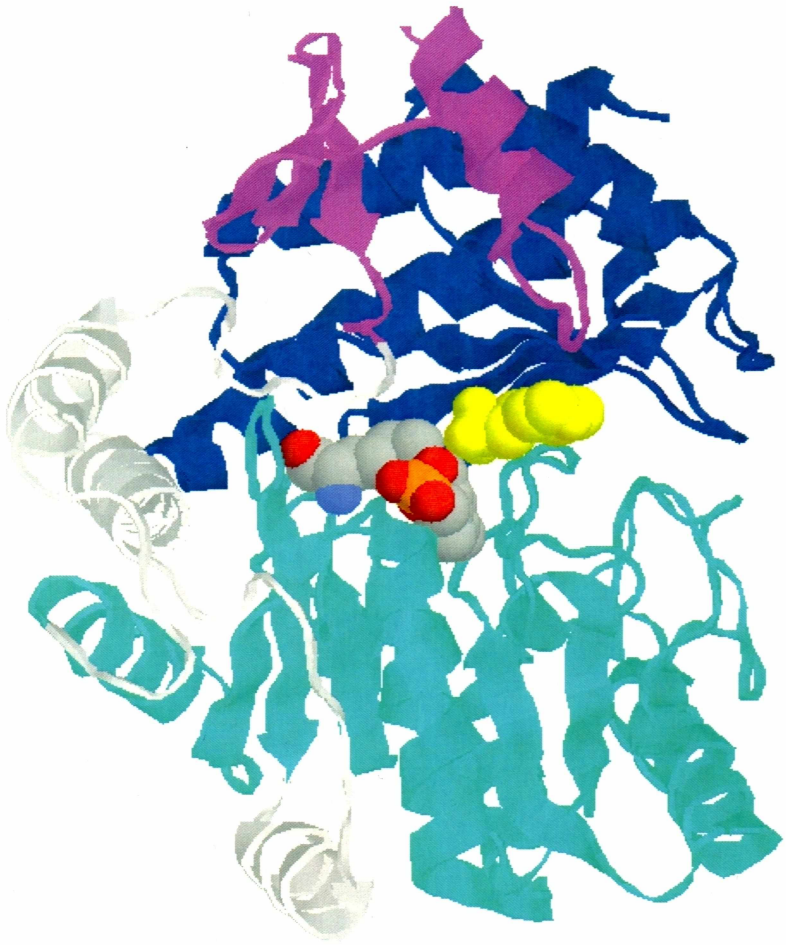

Figure 1.3b – Three dimensional representation of the helices and β-sheets in DGD. Note: This figure was produced by Dr. John Keller, University of Alaska Fairbanks. Protein data bank file 1D7U. Dgd subunit with l-[3-hydroxy-2-methyl-5-phosphonooxymethyl-pyridin-4-ylmethyl]-N,O-cycloserylamide bound at the active site. Image created with Rasmol v. 2.6.

DGD is a dimer of dimers and exists as a tetramer. The tetrameric interface is three times smaller than the dimeric interface, and it is formed by interactions between helix 6 and its N-terminal associated loop with their symmetrical mates in adjacent strands. About ten residues from each subunit participate in the formation of the tetramer.

DGD has two alkali metal binding domains, a predominantly potassium binding site near the active site and a sodium site associated with the surface. The close proximity of site one to the active domain has been proposed to account for the dependence of DGD function on potassium. The importance of this interaction is further indicated by structural disruption when sodium is bound to this site which inhibits enzyme activity as determined by Lamartiniere et al. in 1971. Like other PLP binding enzymes such as tryptophanase and tyrosine phenol lyase, cations also play an important role in the regulation of DGD enzyme activity. However, ion dependence is not absolute because high concentrations of PLP can restore DGD activity in the absence of cations (Hohenester et al., 1994). (*12*)

In the DGD crystal structure, the potassium ion is liganded by interactions with five amino acids (Asp307, Leu78, Thr303, Val305, and Ser80) and a water molecule contributing hydrogen bonds and other electrostatic interactions. The sodium ion coordination interactions are contributed by the carboxylate group of Asp307 and the carbonyl atoms of Leu78 and Val305. Differences in the interaction with water molecules contribute to the different geometries existing between the potassium and the sodium binding sites. The exchange of ions, particularly at the potassium site, will affect the conformation of the active site reside Tyr301 and other distal regions.

Enzyme activity is dependant on the following critical amino acids and the generation of reactive intermediates. (*i*) The pyridine nitrogen of the PLP forms a strong hydrogen bond / salt bridge with Asp243 which hydrogen bonds to His139 and Asn113. This interaction enables the chemical change of PLP into an aldimine via Lys272. (*ii*) It is

proposed that decarboxylation of L-isovaline with the carboxylate group of L-isovaline perpendicular to the PLP ring plane is important for catalysis . The methyl group would point up towards Tyr301 and Met141; the ethyl group of L-isovaline would then lie against the Trp138 indole ring. The transamination of L-isovaline would put the C^{α}-H bond perpendicular to the PLP ring plane and on the same side as Lys272. The Lys272 would act as a general base catalyst in analogy to the aspartate aminotransferase. (*iii*) Crystallography indicates that the active site is unique in having three subsites that contribute to catalysis.(*13*) Subsites A and B accommodate carboxylate groups and are thought to be active in decarboxylation. In contrast, subsite C is proposed to facilitate transamination to L-amino acids (Figure 1.1).

In conclusion, Toney et al. found that DGD has two alkali metal binding domains that regulate enzyme activity and explain the inhibitory effects of sodium on DGD. A detailed description of a monomer and the tetramer as a whole was presented based upon crystal structures of DGD, and lead to a proposed mechanism for DGD transamination and decarboxylation in the same active site.

1.7 DGD – a Decarboxylating Transaminase or a Transaminating Decarboxylase?

Since the DGD catalyzes amino transfer and decarboxylation, many have wondered if DGD was first an aminotransferase that gained the ability through evolution to decarboxylate, or vice versa. In 1990, Keller et al. found that the DGD amino acid sequence deduced from the dgd gene was homologous with the amino acid sequence found for mammalian ornithine aminotransferase.(*1*) It was also determined that the

active site of DGD was similar to that of other aminotransferases. At the optimum alignment of the DGD and the rat ornithine aminotransferase, only one pair of lysines align. These lysines are K272 of the DGD sequence and K292 of the rat ornithine aminotransferase. It was shown in 1986 by Simmaco et al,. that K292 is in the active site of ornithine aminotransferase.(*14*) In 1990 Keller et al. showed that K272 was in the active site of DGD. Keller et al. also reported that the amino acid sequences on both sides of these lysine residues are conserved in several aminotransferases. In addition to the comparison of these two enzymes, DGD was compared to several other decarboxylases through several database searches, and no significant similarities were found between DGD and other decarboxylating enzymes. Keller et al. also noted that there was no active site histidine-lysine pair in DGD which is found in all known prokaryotic PLP dependent decarboxylases. In 1991, it was found that the polyalanine model of DGD showed a fold similar to aspartate aminotransferase and pyruvate aminotransferase.(*13*) In addition, in 1995 Toney et al. performed an overlay of the DGD structure with the structure of aspartate aminotransferase after the crystal structure of DGD was found.(*11*) For the large domain of DGD, all seven of the pleated sheet strands are closely related, and four out of nine of the DGD helices show overlap with aspartate aminotransferase. Also, all three of DGD's helices in the small domain are very similar to the small domain of aspartate aminotransferase. In addition, the active sites of the two molecules are very close in structure with exactly the same positions, as stated by Toney et al., of the PLP pyridine nitrogen atom, the aspartate carboxylate group that is its hydrogen bond-salt partner, and the imidaxole nitrogen atom that hydrogen bonds to this

carboxylate group. This information strongly implies that DGD is more than likely a "decarboxylating aminotransferase" and not a "transaminating decarboxylase".

Part II – Fluorinated Amino Acids

1.8 Fluorinated Amino Acids as Enzyme Inhibitors

The use of fluorinated amino acids can give important clues to the mechanism of an enzyme with the parent substrate. Substituting fluorine in place of hydrogen in an amino acid that is a substrate for an enzyme can cause mechanism-based inactivation of the enzyme. Since fluorine does not cause any significant steric changes in the enzyme, important reactions of the enzyme can be evaluated based on the mechanism of the fluorinated inhibitor. Fluorinated analogues of amino acids are useful because they can stop the reaction of an enzyme just prior to the release of the substrate. Analysis of this complex can give rise to several mechanistic clues that can be extrapolated back to the normal reaction. The following descriptions give several examples in which fluorinated amino acids were used to gain information on the enzyme's reaction with the normal substrate.

1.9 Fluorinated Amino Acids and Decarboxylases

In 1970, Unkeless and Goldman found that γ-aminobutyric acid metabolism in the nervous system can be inhibited by use of the fluorinated analogue of glutamate.(*15*) Glutamate decarboxylase reacts with L-γ-glutamate to from γ-aminobutyric acid

(GABA), and the fluorinated analogue of L-γ-glutamate reacts with glutamate decarboxylase to form α-fluoro-γ-aminobutyric acid (F-GABA). It was found that the L isomer of the fluorinated glutamate had a higher affinity for the enzyme than the D isomer. This was no surprise since the L isomer of glutamate is the normal substrate for glutamate decarboxylase. The K_m was determined to be 5×10^{-3} M which is the same as that for L-glutamate. Also, F-GABA can inhibit GABA uptake. These findings provide a beginning to the use of these compounds in determining the use of GABA in the brain.

In 1979, Sato et al. found that β-chloro-L-alanine inactivates α-aminoisobutyrate decomposing enzyme.(*16*) β-chloro-L-alanine is a substrate for the AIB decomposing enzyme when an α-ketoacid is absent. Equimolar production of chloride, ammonia and α-ketoacid were observed. The production of chloride suggested that the ketoacid produced was pyruvate and not chloropyruvate which would be the product if transamination had occurred. The production of pyruvate was confirmed by spectral analysis. Thus, it is likely that α,β-elimination is the mechanism of this reaction. Sato et al. also concluded that the D-form of β-chloro-L-alanine is not a substrate for the AIB decomposing enzyme. Since it was found that the reaction does not occur in the absence of PLP, this α,β-elimination is PLP dependent. The AIB decomposing enzyme has a higher affinity for β-chloro-L-alanine than for AIB or alanine. A time course of the formation of pyruvate from the inactivation of the AIB decomposing enzyme with β-chloro-L-alanine showed a small deviation from a straight line. Also, the relationship between the loss of activity and α,β-elimination was linear. It was reported that AIB decomposing activity, transamination, and α,β-elimination were all three lost in parallel.

From these results, Sato et al. concluded that one of the intermediates of α,β-elimination was responsible for the inactivation of the AIB decomposing enzyme, and an identical active site was utilized for each of the three reactions of the AIB decomposing enzyme.

In 1986, Hayashi et al. found that (S)-α-fluoromethylhistidine was an inhibitor of *Morganella morganii* AM-15 histidine decarboxylase.(*17*) Histidine decarboxylase is a PLP dependent enzyme, and the holoenzyme was inactivated by (S)-α-fluoromethylhistidine, but the apoenzyme was not inhibited by (S)-α-fluoromethylhistidine. It was found that a single molecule of (S)-α-fluoromethylhistidine inhibits one enzyme subunit under optimal conditions. The k_{inact} of the reaction was found to be 32.2 min^{-1}. Also, it was determined that L-histidine, the normal substrate, protects the enzyme against inactivation. These results indicate that (S)-α-fluoromethylhistidine is a mechanism-based inhibitor of histidine decarboxylase. Once the inhibitor is bound to the enzyme, it can be removed by the addition of heat or urea. The released product was not characterized. However, they did find that the released product contained a tritium label if the inhibitor was tritiated, α-fluoromethyl-[^{3}H] histidine. Hayashi et al. proceeded to react α-fluoromethyl-[^{3}H] histidine with enzyme reduced by sodium borohydride and carboxymethylated. After the reaction was complete, the complex was trypsinized and the peptides were separated by RP-HPLC. Only one peak contained radioactivity, referred to as T-10m, and it contained 85% of the original amount of tritium added to the reaction. This indicated that there was only one modification made to the enzyme by the inhibitor. A ratio of one inhibitor: one peptide: one PLP was found. A native histidine decarboxylase was carboxymethylated

and digested with trypsin and subjected to RP-HPLC for comparison. The peptide maps of both the carboxymethylated enzyme and inhibited enzyme were essentially the same. The carboxymethylated enzyme had a peak very similar to the radioactive peak in the inhibited enzyme peptide map, referred to as T-10. That peak was collected and purified for analysis. Upon sequencing of T-10 and T-10m, it appeared that they contained the same amino acid sequence except for one amino acid, serine was in the second position in T-10 and the second position in T-10m was unidentifiable. However, the second position of T-10m did contain radioactivity. Thus, it was concluded that serine is the modified amino acid in the inhibited histidine decarboxylase.

In 1995 Reguera et al. produced fluorinated analogues of L-ornithine that inhibit ornithine decarboxylase.(*18*) One irreversible inhibitor of ornithine decarboxylase is α-difluoromethylornithine (DFMO). DFMO was utilized as a clinical agent for the treatment of trypanosomiasis (sleeping sickness). Trypanosomiasis is an infectious parasitic disease carried by tsetse flies and characterized by inflammation of the brain and the covering of the brain (meninges). This paper demonstrates the relevance of the use of fluorinated inhibitors in human disease treatments.

1.10 Fluorinated Amino Acids and Transaminases

In 1975, Relimpio et al. found that α-trifluoromethyl-DL-alanine is an inhibitor of aspartate transaminase, a PLP dependent enzyme.(*19*) The inhibitor, α-trifluoromethyl-DL-alanine, was produced in the form of a fluorinated amino acid-PLP complex. The complex was reacted with the enzyme at room temperature. The complex

completely inactivated the enzyme. When the racemic inhibitor was used, only one half of the amount of inhibitor was used by the enzyme suggesting that only one isomer is able to bind to the active site of aspartate transaminase. It was found that the fluorinated inhibitor could not be displaced by the cofactor or any amino acid combinations suggesting that there is a high affinity between the inhibitor and enzyme. The inhibitor was not released upon dialysis or column chromatography (Sephadex G-25). However, the α-trifluoromethyl-alanine can be displaced by treatment with potassium phosphate buffer, pH 6.0. This treatment can completely restore catalytic activity. Since the bond between the enzyme and inhibitor complex is easily reversible, it is safely concluded that this is not a covalent bond.

In 1981, Wang et al. found that D-fluoroalanine is a mechanism-based inhibitor of serine transhydroxymethylase, a PLP dependent enzyme.(*20*) Serine transhydroxymethylase can catalyze the slow transamination of D-amino acids, namely D-alanine, to form pyruvate, PMP, and apoenzyme. The fluorinated analogue of D-alanine, D-fluoroalanine, acts as a suicide substrate for serine transhydroxymethylase. Wang et al. found that D-fluoroalanine inhibits serine transhydroxymethylase purified from rabbit and lamb liver in the presence of tetrahydrofolate. The K_m of D-fluoroalanine is high at 50 mM, the same as that of D-alanine, which suggests that this fluorinated amino acid would not be useful for *in vivo* studies of inactivation of liver cell serine transhydroxymethylase because the inhibitor would not have a higher affinity for the enzyme than the natural substrate. Although D-fluoroalanine would not make a clinically

useful mechanism-based inhibitor, it does have utility as an antibacterial agent since it can inactivate alanine racemases.

In 1996, Kato et al. found that S-(1,1,2,2-Tetrafluoroethyl)-L-Cysteine is an inhibitor of aspartate aminotransferase and alanine aminotransferase.(*21*) S-(1,1,2,2-Tetrafluoroethyl)-L-Cysteine (TFEC) is a xenobiotic which may result in an increased risk for some cancers. Kato et al. hypothesized that the reason for the toxicity of TFEC is due to inhibition of important PLP dependent enzymes such as aspartate aminotransferase and alanine aminotransferase. After performing several experiments, they found that TFEC inactivates aspartate aminotransferase in purified pig heart, rat brain, and rat kidney. These inactivations are enhanced in the presence of α-ketoglutarate, and very little pyruvate is detected. These results suggest that the reaction of the PLP-TFEC complex to PMP and the keto form of the TFEC, transamination, competes favorably with the conversion to PLP and pyruvate. Also, TFEC inactivates alanine aminotransferase in purified pig heart in a time dependent fashion, and L-glutamate protects this activation. Kato et al. showed that PLP dependent enzymes, aspartate aminotransferase and alanine aminotransferase, are indeed inhibited by TFEC which may cause an increases in certain types of cancer. These findings justify further investigation of TFEC as a carcinogen.

1.11 A Mechanism-Based Inhibitor of DGD

In 1979, Keller and O'Leary found an irreversible mechanism-based inhibitor of the *Pseudomonas cepacia* α-dialkylamino acid transaminase, known today as DGD.(*3*) As

stated previously, the normal substrate for DGD is 2-aminoisobutyrate (AIB), also known as 2-methylalanine. The enzyme is a PLP dependent decarboxylating aminotransferase. Decarboxylation of AIB results in the formation of carbon dioxide, acetone, and the amino form of the cofactor (PMP). Then, transamination of the pyruvate forms L-alanine and regenerates the cofactor in the PLP form. Keller and O'Leary found that (+)-3,3,3-trifluoro-2-aminoisobutyrate (F3AIB) inhibits DGD in a time dependent fashion in the presence of PLP. The reaction with the inhibitor decarboxylates the substrate, and then covalently binds to the active site of DGD, completely inactivating the enzyme. The apoenzyme is not inactivated by F3AIB. The first order rate constant was found to increase with increasing concentrations of F3AIB. Upon dialysis of the inhibited enzyme the activity could be not restored even after several hours which suggest a covalent attachment of the inhibitor to the enzyme. The product of the natural reaction, L-alanine, is a known competitive inhibitor with the natural substrate, AIB. L-alanine is also a competitive inhibitor of F3AIB. In addition, there is also some protection of the enzyme provided by AIB.

Keller and O'Leary performed experiments with [1-^{14}C] F3AIB so that the molar ratio of inhibitor decarboxylated to enzyme monomer inactivated could be determined.(*3*) Upon liberation of [^{14}C] CO_2 from a known amount of enzyme, the labeled CO_2 was trapped and quantified. A value of 10 was determined for the ratio of decarboxylated inhibitor to enzyme monomer inactivated.

Keller and O'Leary proposed that the enzyme is inactivated at the active site based on their observations that AIB and L-alanine protect the enzyme from inactivation and that

the inhibitor is decarboxylated with a ratio of 10 moles of CO_2 to each monomer inactivated. In addition, they also suggested that the inhibitor covalently attaches to the enzyme. Thus, F3AIB is a mechanism-based suicide inhibitor of DGD.

1.12 *R* Isomer of F3AIB, a Better Suicide Inhibitor of DGD than the S Isomer

In 1982, Keller found that the (+)-isomer of F3AIB is more active against the enzyme, dialkylamino acid transaminase than the (-)-isomer of F3AIB.(*22*) The (-)-isomer has been found to inactivate the enzyme slowly or not at all. When the enzyme is reacted with racemic F3AIB the (-)-isomer can get into the active site of the enzyme and inhibit the (+)-isomer from inactivating the enzyme thus the (-)-isomer is a competitive inhibitor. After the (-)-isomer disassociates from the enzyme, the (+)-isomer can move into the active site and completely inactivate the enzyme.

In 1984, Keller and Day found that the (+)-isomer of F3AIB corresponded to the *R* configuration of F3AIB (Figure 1.4).(*22*) Through analysis of the crystals by X-ray diffraction studies of (R)-N-chloroacetyl-(+)-3,3,3-trifluoro-2-aminoisobutyric acid, Keller and Day were able to show that D-alanine and (R)-N-chloroacetyl-(+)-3,3,3-trifluoro-2-aminoisobutyric acid both have the same configuration of methyl, amino acid, and carboxylate groups. These findings support the previous conclusions of Bailey et al. that the D- and L-alanine are both substrates for dialkylamino acid transaminase; however, they produce different results when processed by the enzyme. D-alanine is decarboxylated and transaminated to acetaldehyde while L-alanine is transaminated to pyruvate. These findings also support the finding by Keller

et al. that inactivation of the transaminase by F3AIB is accompanied by decarboxylation. From this evidence, Keller et al. concluded that F3AIB and the normal substrate have similar binding patterns DGD thus F3AIB can be referred to as a mechanism-based suicide inhibitor of DGD.

R-2-trifluoromethylalanine S-2-trifluoromethylalanine

Figure 1.4 – Isomers of F3AIB showing the R and the S configuration.

Part III – Mass Spectroscopy

1.13 Mass Spectroscopy of Modified Proteins

Mass spectroscopy is an extremely useful tool in analyzing peptide mixtures that are a result of enzyme digestions.(*23*) The reason that LC/MS (Liquid Chromatography/Mass Spectroscopy) has become such a powerful tool is because the HPLC portion of the instrument separates the sample and the mass spectrometer can immediately analyze the samples at femtomole levels. LC/MS can be used to confirm the sequence of proteins, and it can be used to determine the location of a change in an amino acid sequence. Davis et al. reported several examples of the utility of LC/MS. One example is the use of

trypsin and LC/MS/MS to analyze a human hemoglobin variant. From this analysis, Davis et al. found that one of the peptides in this protein had a substitution of Lys for Gln. This substitution had been previously known; however, Davis et al. fully characterized the variant and confirmed the substitution with a single LC/MS/MS run.

Also, instead of comparing peptide maps and analyzing retention times the MS/MS will analyze each peak and determine the mass. Thus, one can determine if a HPLC peak is at a different retentions time due to run-to-run variations or if there is indeed a different peptide in the sample, such as a peptide with a covalently bound inhibitor that caused the retention time to shift.(*24*)

In 2001, Chen and Frey found the presence of an aldimine linkage between PLP and a lysine residue in the active site of lysine 2, 3-aminomutase (LAM).(*25*) LAM catalyzes the interconversion of L-lysine and L-β-lysine. LAM is a PLP dependent enzyme although the mechanism by which it utilizes PLP is very different than the typical PLP dependent enzymes. PLP dependent enzymes usually involve the PLP binding to the active site by forming an aldimine link between the carbonyl group of the cofactor and the ϵ-amino group of the active site lysine. The amino group of the substrate replaces the ϵ-amino group of the active site lysine and the reaction proceeds via stabilization of amino acid carbanions. The LAM reaction is unique because it utilizes a radical rearrangement mechanism. The common PLP binding motif S-X-X-K (PLP) was found in LAM. Also, the amino acids flanking this motif were found to be similar to the PLP binding sites of aspartate aminotransferases. Spectral changes upon reduction with sodium borohydride suggested that there was an aldimine linkage. To determine if an

active site lysine was involved in this aldimine linkage, $NaBH_4$ reduced LAM and nonreduced LAM were carboxymethylated, denatured, digested with trypsin, and then analyzed by HPLC with a C18 column. Upon spectral analysis, the peptides from the reduced enzyme showed an absorption band at 280 nm and 325 nm, but the non reduced enzyme showed no absorption band at 325 nm. This indicates that there was a loss of PLP in the non reduced enzyme. The chromatograms from the HPLC were compared; the chromatograms were the same except for the $NaBH_4$ reduced LAM showed a peak at 23.7 m whereas the nonreduced enzyme had no peak at this retention time. This peak was subjected to analysis by ESI/MS. The molecular mass of this peptide was found to be 3860.64 ± 0.26 Da. This is equal to the mass of a 36 residue peptide of LAM (3629.05 Da) plus 231.14 mass units for the attachment of PLP. The peptides from the nonreduced and the reduced LAM were then analyzed with LC/MS. A peptide with a mass of 3859.98 ± 0.18 Da was found in the reduced enzyme, but it was not found in the nonreduced enzyme. However, two peptides with masses of 1974.36 ± 0.41 Da (residues 326-346) and 1672.22 ± 0.30 Da (residues 347-361) were identified in the nonreduced enzyme; however, they were absent in the LC/MS of the reduced enzyme. These two peptides are two halves of the larger peptide found in the reduced enzyme which suggests that Lys 346 is covalently modified by PLP thus making it unrecognizable as a trypsin cutting site which results in two peptides remaining together. In addition, the peptides were sequenced by MS/MS which also confirmed a 231 mass attachment to Lys 346. These experiments demonstrate that ESI/MS, LC/MS, and MS/MS can distinguish between a nonmodified peptide and a modified peptide.

In 2001, Li et al. found a mechanism-based inactivator of S-adenosylmethionine decarboxylase *in vivo*, and through the use of MS they showed that this inactivation correlates with a posttranslational modification of the α subunit of the enzyme.(*26*) S-adenosylmethionine decarboxylase (AdoMetDC) is required for the biosynthesis of spermidine and spermine. These studies were conducted using enzymes from *E. coli*, *Saccharomyces cerevisiae*, and *Salmonella typhimurium*. The enzyme was synthesized as a proenzyme which is cleaved posttranslationally to form an active enzyme. The mature enzyme is composed of a β subunit and a α subunit. AdoMetDC contains a covalently bound pyruvoyl end group within a α subunit that is required for the enzyme to be active. It is likely that the decarboxylation of AdoMetDC proceeds via formation of a Schiff base between the pyruvoyl group and the amino group of the substrate. Also, it is known that the product of the reaction which is decarboxylated S-adenosylmethionine (dcAdoMet) can inhibit the enzyme. Upon production of AdoMetDC, Li et al found that a large amount of the enzyme was inactive. Thus, the purified enzymes were trypsinized and separated via HPLC with a C3 or a C18 column. The separated peptides were then analyzed by LC/MS/MS. In addition to two expected peaks each representing a subunit, there were one or two additional peaks at masses 57 ± 1 and 75 ± 1 Da. The unexpected peaks accounted for 30-70% of the α subunit which suggested that there was extensive modification of the enzyme *in vivo*. Li et al. also found that the pyruvoyl groups of the α subunit can be transaminated to alanine. This reaction is similar to that of the decarboxylation-dependent transamination of pyridoxal phosphate dependant enzymes. Upon digestion of the *E. coli* enzyme with trypsin and peptide mapping by LC/MS, a

modification of Cys 140 was revealed. MS/MS studies indicated a +76 modification of Cys 140. Li et al. speculated that the modification was caused by the reversible binding of the product, dcAdoMet, which then causes an irreversible modification of the enzyme. Assays for dcAdoMet in trichloroacetic acid cell extracts did not show an increase in dcAdoMet. The loss of enzyme activity correlates with the increase in the modified enzyme, but the loss of activity is greater than the amount of the modification. These results would be expected if modification of only one or two of the four subunits inactivated the enzyme. Thus, Li et al. concluded that the inactivation of the enzyme proceeds via the occasional transamination reaction that is followed by alkylation of the Cys 140 sulhydryl group which completely inactivates the enzyme.

Chapter 2 – Materials and Methods

Part I – Materials

An autoclave was used to sterilize solutions. A Sorvall RC 5B Plus centrifuge with a Super-lite GSA rotor and a SS-34 rotor was used for centrifugation. A Hewlett Packard Diode Array UV spectrophotometer was used with 1 cm plastic cuvettes for protein concentration assays and a 0.5 cm quartz cuvette was used for kinetic assays. Petri dishes, toothpicks, 15 mL culture tubes, and a shaker were used to grow *E. coli*. A W225 Heat Systems Ultrasonics sonicator, ¼ inch dialysis tubing, a Gilson peristaltic pump, detector, and fractionator, and a 2.5 x 12 cm column were used in the purification process. The Beckman HPLC contained a model 126 solvent module, a 168 detector, a 508 Autosampler, and System Gold Version 1.7. The column utilized was an Alltech Econosphere C18 5 μ, 15 mm x 4.6 mm column with an Alltech 7.5 mm x 4.6 mm column guard, and an Ansys flow-through design back pressure regulator. Solvents were degassed. Also, a Labconco centravap system was used to dry HPLC fractions. Finally, samples were analyzed on a VG or Kratos multi-sector tandem mass spectrometer at the Washington Univ. Center for Biomedical and Bioorganic Mass Spectrometry.

E. coli JM109 carrying the plasmid pJKDGD-A2.2 was used to extract and purify DGD. Tryptone, yeast extract, NaCl, agar, ampicillin, triethanolamine, glycerol, monobasic and dibasic potassium phosphate, isopropyl β-D-thiogalactopyranoside (IPTG), tris base, 2-methylalanine, pyruvate, pyridoxal 5'-phosphate (PLP), and KCl

were utilized in media for growing *E. coli* and in reaction buffers. NaOH and HCl were used to change the pH of solutions. Bovine Serum Albumin (BSA) and Bradford Reagent were used to determine protein concentrations. Ammonium sulfate was used to precipitate out undesired proteins. Bio Rad ready made SDS-PAGE 12% Tris-HCl with 10 wells and a 30 μL comb and coomassie blue were used for SDS-PAGE analysis. Bio Rad P-6D6 resin and Supelco DEAE-650M resin was required for column chromatography. Sodium borohydride (Altech, Inc) was used to reduce DGD, and L-1-tosylamide-2-phenylethyl chloromethyl ketone (TPCK) trypsin was needed to cleave DGD. HPLC grade acetonitrile and formic acid were the HPLC solvents used. Finally, *R* (+) isomer of F3AIB and racemic F3AIB-d_3 were used to inhibit DGD.

Part II - Methods

2.1 DGD Purification

The plasmid carrying the DGD gene was grown in *E. coli* so that the DGD protein could be extracted and purified through sonication, ammonium sulfate precipitation, dialysis, and ion-exchange chromatography for further studies of this enzyme.

a. Cell Growth

DGD was purified from *E. coli* JM109 carrying the plasmid pJKDGD-A2.2 which contains the DGD gene (Figure 2.1).

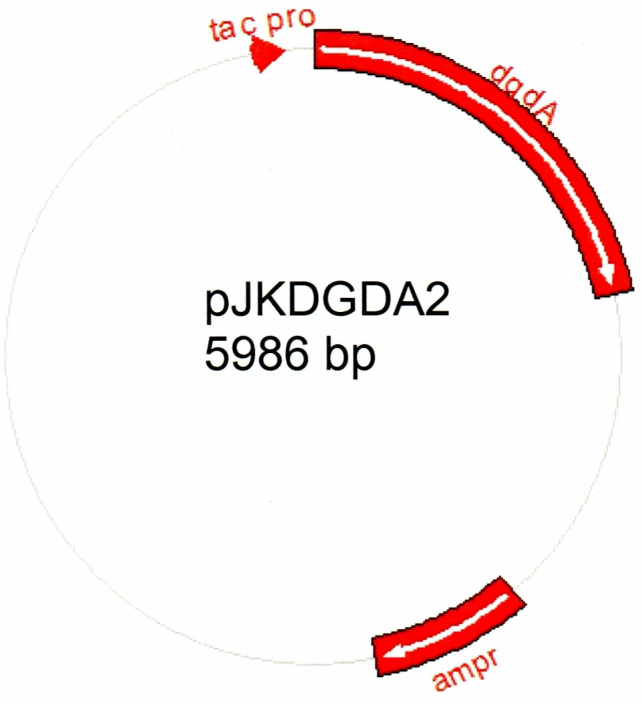

Figure 2.1 – pJKDGD-A2.2 plasmid. This plasmid carries the DGD gene.

The purification was done in two batches. JM109 pJKDGD A2.2 was plated on Luria Broth (LB) consisting of sterile 1% tryptone, 0.5% yeast extract, 1% NaCl, 0.75% agar, and 0.1 mg/mL ampicillin in water (LB-AMP plates). The plates were incubated at 37°C overnight. Then, an isolated colony was removed with a sterile toothpick and placed into 0.2 mL of sterile LB (1% tryptone, 0.5% yeast extract, 1% NaCl, and 0.08 mg/mL ampicillin in water). Approximately 0.028 mL of the colony in LB was placed into seven 15 mL culture tubes containing 2.5 mL of sterile LB each. The tubes were shook at 200 RPM at 37°C for approximately 12 h. One tube was preserved at -70°C for later use. Then, two tubes were placed into a Fernback flask containing 900 mL of Terrific Broth

(1.2% tryptone, 2.4% yeast extract, 0.004% glycerol, 0.17 M monobasic potassium phosphate, 0.72 M dibasic potassium phosphate), plus 0.05 mg/mL ampicillin, and 0.5 mM isopropyl β-D-thiogalactopyranoside (IPTG). IPTG is a synthetic inducer of the lactose operon. It induces the operon by vastly decreasing the affinity of the repressor for DNA. The inactivation of the repressor stimulates transcription because it removes the steric block of the repressor-inducer complex. Next, three Fernback flasks were shook for 10 h at 37°C. The cells were grown to an OD at 600 nm of 0.86. This was determined by taking the UV spectrum of 0.2 mL of cells diluted with 1.5 mL of water.

b. Protein Assay

A standard curve was made by taking readings on a Hewlett Packard Diode Array UV spectrophotometer at 595 nm with 1 cm plastic cuvettes consisting of 0, 5, 10, 20, 30, and 40 μg of bovine serum albumin (BSA) in 1.5 mL of Bradford Reagent. (*27*) The Bradford method utilizes a dye that binds proteins and causes a change in color which results in a change in absorbance. Protein absorbance versus protein concentration was plotted for the determination of unknown protein concentrations (Figure 2.2). The protein concentration of a protein can be determined by the absorbance when the absorbance is plotted on the graph in figure 2.2.

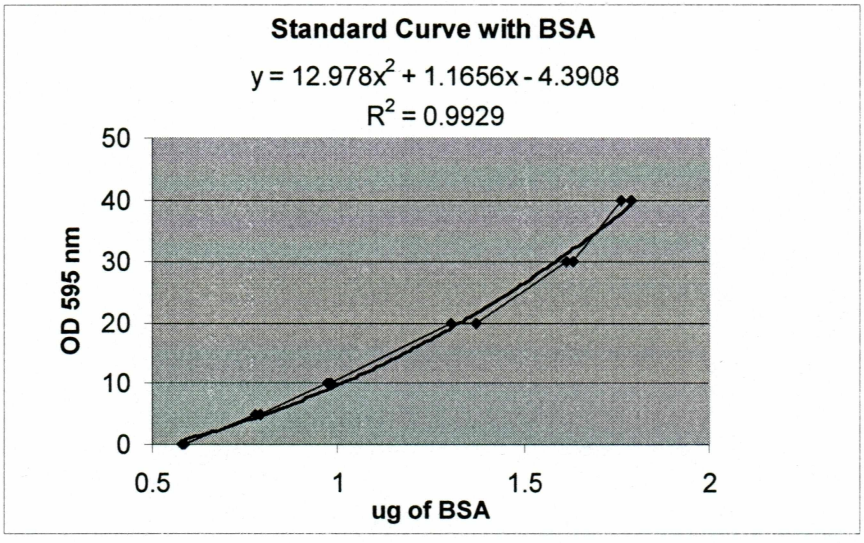

Figure 2.2 – Protein concentration standard curve with BSA. The absorbance of an unknown protein can be plotted in this graph to determine the protein concentration.

c. Ammonium Sulfate Precipitation and Dialysis

Next, the cells were centrifuged in a Sorvall RC 5B Plus centrifuge with a Super-lite GSA rotor which was precooled to 4°C, unless otherwise noted, at 6,000 RPM for 10 min. The supernatant was discarded; the resulting cell pellet weighed 23.5 g. The sonication buffer consisted of 30 mM Tris, 50 mM KCl, 50 mM NaCl, 1 M ammonium sulfate, 1.5 mM 2-methylalanine, 2.7 mM pyruvate, and 20 μM PLP at pH 7.9. The cells were resuspended in 150 mL of sonication buffer, and stirred on ice until the mixture was at 4°C. The cells were sonicated six times in 5 min intervals with a W225 Heat Systems Ultrasonics sonicator. They were allowed to cool to slightly below 4°C in between sonication periods, and they were never allowed to exceed 7°C throughout the sonication process. The absorbance of the cells was taken at 595 nm after each sonication period

from the 2nd to the 6th by removing 5 μL and placing it into 1.5 mL of Bradford Reagent and reading the absorbance (Table 3.1) (*27*). After the cells were sonicated, they were spun at 12,000 RPM for 20 min. After centrifugation, 4 μL of the supernatant was removed and placed into 1.5 mL of Bradford Reagent, and the absorbance was taken at 595 nm (Table 3.1). The supernatant was poured off and 113 mL of a 3.8 M ammonium sulfate solution was added to precipitate out undesired proteins. The solution was magnetically stirred on ice, and then centrifuged at 10,000 RPM for 20 min. The supernatant was poured off, and the pellet was resuspended in 100 mL of dialysis buffer on ice. The dialysis buffer consisted of 20 mM triethanolamine, 5 mM KCl, 5 mM NaCl, 2 mM pyruvate, 1 mM 2-methylalanine, and 18 μM PLP at pH 7.9. The pellet was not shaken or stirred, but it was allowed to dissolve slowly on ice. When the pellet was completely dissolved, 4 μL were assayed for protein concentration by the Bradford method. The dissolved pellet was placed in 1 ¼ inch dialysis tubing that had been soaking in deionized water for 1 h. The tubing was clamped shut and placed in a 2 L graduated cylinder with approximately 1.9 L of dialysis buffer and a 1.5 inch magnetic stir bar. The tubing was stirred at 4°C overnight. The following day, the contents of the dialysis tubing was centrifuged at 12,000 RPM for 20 m at 4°C.

d. Ion-Exchange Chromatography

A Gilson peristaltic pump, detector, and fractionator were used. The Supelco DEAE-650M resin, 75 mL, was added to 250 mL of water and packed into a 2.5 x 12 cm column. Approximately, 125 mL of a 5 mM NaCl and 5 mM KCl buffer was run through the column prior to adding the sample. Then, the sample was loaded and followed by a

gradient of a low (5 mM) to a high (250 mM) KCl and NaCl concentration. The detector was set to read at 290 nm, and the sample was pumped through the column at a rate of 2 mL/min. Then, 4 mL fractions were collected. Fractions were analyzed by placing either 3, 4, or 10 μL into 1.5 mL of Bradford Reagent and taking the absorbance at 595 nm. The protein concentration was calculated and plotted using the absorbance data and the equation of the line from the standard curve (Figure 3.1a). Also, a SDS-PAGE was performed via the Bio Rad protocol with a Bio Rad ready made 12% Tris-HCl gel with 10 wells and a 30 μL comb (Figure 3.1b). The only exception to the Bio Rad protocol was that the concentration of the Coomassie Blue staining solution was reduced to 0.05% to reduce blue background in the gel.

e. Activating Column

Finally, an activating column was run to load the DGD with the cofactor, PLP. The column consisted of 3 g of Bio Rad P-6D6 resin in 50 mL of 50 mM potassium phosphate buffer pH 7.9 with 2 mM pyruvate, 1 mM 2-methylalanine, and 50 μM PLP. The slurry was allowed to hydrate for 30 m at room temperature. Then, a 1.5 x 12.5 cm column was packed with the resin. The column was equilibrated with potassium phosphate buffer. The detector was set to 290 nm, and the sample was pumped through the column at a rate of 1 mL/min. The sample was eluted in 50 mM potassium phosphate buffer pH 7.9 with 2 mM pyruvate, 1 mM 2-methylalanine, and 50 μM PLP in 3 mL fractions. The fractions were analyzed spectrophotometrically at 595 nm in 1.5 mL of Bradford Reagent.

The protein was assayed for the uptake of the substrate, 2-methylalanine. First, a scan of the enzyme alone is taken, then the enzyme is reacted with the substrate and another scan is taken. The scan should show the change of PLP into PMP. This was done by taking a scan of 100 mM dibasic potassium phosphate pH 7.0 and 100 μL of purified DGD. The total volume of the enzyme substrate reaction was 0.5 mL. Next, 100 mM 2-methylalanine was added and the mixture was scanned again (Figure 3.2).

Finally, fractions 18-23 from the column were combined and concentrated using Centricon-30 Concentrators in 50 mL centrifuge tubes. Before and after the concentration of the enzyme, the protein concentration was determined via the Bradford method described above (Table 3.2). The pooled fractions had a pale yellow color due to the presence of DGD. The Sorvall RC 5B Plus centrifuge with a SS-34 rotor was spun at 5,000 RPM for 20 min three times. The rotor was precooled to 4°C. After the fractions were combined, a kinetic assay was run on the purified DGD (Figure 3.3). This assay observes the loss of pyruvate as it is consumed by the enzyme. Thus, as the pyruvate is lost the absorbance decreases. To perform this assay a reaction buffer was prepared which consisted of 50 mM dibasic potassium phosphate pH 7.0, 2 mM pyruvate, 20 mM 2-methylalanine, and 10 μM PLP. The purified DGD, 5 μL, was added to 1 mL of the reaction buffer and time points were taken every 2 s at 222 nm in a 0.5 cm cell. The assay ran for 180 s. Finally, the protein was stored at -70 °C in 0.5 mL aliquots.

2.2 Reduced DGD Purification

Another activating column was run to ensure that the enzyme was loaded up with the cofactor, PLP (see section 2.1.e for method). Then, the cofactor-bound DGD was reduced by sodium borohydride to form a covalent bond between the cofactor and the enzyme. The covalent bond will not break when the enzyme is analyzed by HPLC and/or LC/MS/MS. This allows the amino acid site of attachment of the PLP to be studied.

First, a total of 7 mg of purified DGD was injected onto the column and eluted in 1 mL fractions with potassium phosphate buffer. The three fractions containing the most amount of protein were combined and reduced with 5 mg of sodium borohydride at room temperature for 1 h. The reaction produced a significant amount of bubbles due to the production of hydrogen gas. The combined fractions were analyzed by taking the absorbance at 595 nm of 10 μL of the reduced protein solution mixed with 1.5 mL of Bradford Reagent.

Next, 3 mL of reduced DGD was injected onto another activating column as described above. This time 50 mM potassium phosphate buffer pH 7.9 was used to elute the protein in 1 mL fractions. After all of the fractions were collected, 15 μL of each fraction were put into 1.5 mL of Bradford Reagent, and the absorbances were taken at 595 nm. The fractions with the highest concentration of protein were combined and stored at -70 °C for further experimentation.

2.3 Digestion Conditions

DGD can be cleaved into several peptides by trypsin. If the enzyme was not cleaved, the HPLC would produce a chromatogram with only one peak; however, there are several peaks after digestion of the enzyme which can be collected and analyzed by MS. The same scenario would take place in LC/MS/MS. Thus, cleavage is useful to study an enzyme at the amino acid level.

Several tryptic digest reactions were run to determine the optimal concentration of trypsin required to cleave DGD. The lowest amount of trypsin should be used so that the enzyme does not get over digested. Five reactions were run with 1 mg of purified DGD each, approximately 71 μL. L-1-tosylamide-2-phenylethyl chloromethyl ketone (TPCK) trypsin from Sigma was added at 0, 10, 20, 30, or 40 % of the protein concentration. Trypsin, 2.0mg, was dissolved in 0.5 mL of 0.05 M Tris HCl pH 6.8. The reaction was allowed to run for 21 h at 37 °C with gentle shaking after which an SDS-PAGE gel was run (see section 2.1.d.for method)

After an optimal percent of trypsin to enzyme was determined, another experiment was run to determine if the reduced form of DGD could also be digested by trypsin in the same manner. Prior to digestion, 1 mL of the reduced enzyme was concentrated using a Centricon-30 Concentrator in a 50 mL centrifuge tube. This was done to remove contaminants in the buffer solution. The sample was spun at 5,000 RPM for 20 min three times to concentrate the reduced enzyme. The final concentration of the reduced DGD was 6.1 mg/mL with 90 μL of the protein. Thus, 0.55 mg of protein remained. The

digestion reaction was allowed to run for 21 h at 37 °C with gentle shaking. Another SDS-PAGE gel was run according to the conditions in section 2.1.d.

After the analysis of the DGD and reduced DGD samples, the enzyme was reacted with the *R* (+) isomer of F3AIB, a mechanism-based suicide inhibitor of DGD. Any information that is found from a suicide mechanism-based suicide inhibitor can be extrapolated back to the natural substrate because the mechanisms are the same. So if the enzyme amino acid that interacts with the inhibitor can be determined, it can be assumed that the same amino acid is the attachment site for the natural substrate.

The reactions consisted of 3.5 mg of DGD, 2 mM PLP, 50 mM potassium phosphate pH 7.5, and 10 mM of *R*-F3AIB, which was the last component added to the reaction. The total volume was 1mL, and the reaction took place at room temperature for a total of 5 h. The reaction was analyzed by a kinetic assay with a UV spectrophotometer at the beginning of the reaction, 2.5 h, and 5 h to ensure the complete inhibition of the enzyme. At these time points 100 μL of the reaction was removed and placed into 900 μL of an assay solution as described above (Figures 3.6-3.8).

Also, a racemic deuterated inhibitor (F3AIB-d_3) was reacted with the enzyme in parallel with the protonated inhibitor. This was done for further analysis of the inhibitor reaction. The conditions were identical to those described above for the protonated inhibitor; however, the inhibitor was used at 20 mM instead of 10 mM because the F3AIB-d_3 was purified as a racemic mixture. The results are shown in figures 3.6-3.8.

Next, 1 mg of protein was removed from both reactions and placed into two new eppendorf tubes. Then, 20% trypsin was added to each reaction and the reactions were

allowed to shake gently at 37°C for 40 h. At this time, a SDS-PAGE was performed (results not shown); however, the digestion reaction was not complete so another 20% trypsin was added to each reaction and both reactions were allowed to shake gently at 37°C for another 66 h. Finally, a SDS-PAGE gel was run according to the conditions above (Figure 3.9).

2.4 HPLC

RP-HPLC can be used to separate peptides so that they can be collected and analyzed for the amino acid content by MS. The peptides are separated on the HPLC column by their hydrophobicity. The more hydrophobic a peptide is, the longer it will stay attached to the column. If the DGD peptides are separated by RP-HPLC, they can be analyzed by MS for amino acid and possible inhibitor content. The peak from the peptide with the inhibitor attached to it would only appear in the chromatogram of the inhibited DGD.

A Beckman chromatography system was used to perform RP-HPLC. The RP-HPLC setup consisted of a Beckman 126 solvent module, a Beckman 168 detector, and a Beckman 508 Autosampler. The software was Beckman System Gold Version 1.7. The column was an Alltech Econosphere C18 5 μ, 15 mm x 4.6 mm column. Preceding the column was an Alltech 7.5 mm x 4.6 mm column guard. An Ansys back pressure flow-through regulator was used to collect peaks without air bubbles. The method consisted of a gradient from 0% buffer B to 80% buffer B over 100 min. Then, buffer B was returned to 0% over 8 min. The entire HPLC run took 114 min. Buffer A consisted of 0.2% formic acid and 2.0% HPLC grade acetonitrile in water. Buffer B consisted of

0.2% formic acid in acetonitrile. The solvents were degassed before they were pumped onto the column.

Purified DGD, 2.0 mg, was digested with 4% trypsin for 48 h at 37°C with gentle shaking. The reaction was brought up to 1 mL with Tris HCl pH 7.9 prior to the addition of trypsin. Approximately, 200 µl of the sample was injected onto the RP-HPLC with the autosampler. Several peaks were collected by hand during the RP-HPLC run. Four of these peaks were dried down with a Labconco Centravap system. After that, the samples were rehydrated with 100 µL of water and dried down again to remove all of the formic acid. Finally, the samples were sent for ESI mass spectroscopy (MS) analysis at the University of Washington in St. Louis, MO.

Another tryptic digestion of DGD was performed in tandem with a tryptic digestion of an inhibited DGD. Purified DGD, 3.5 mg, was put into each of two eppendorf tubes, and each reaction was brought up to 1 mL total volume with water. *R* (+) isomer of F3AIB was added at 20 mM to the reaction as the last ingredient. The reaction was allowed to incubate at room temperature for 1 h. Then, 4% trypsin was added to each reaction. The reaction was allowed to shake gently at 37°C for 48 h. Finally, 200 µl of each reaction was injected onto a RP-HPLC column as described above with an autosampler (Figures 3.10-3.11).

2.5 LC/MS/MS

An LC/MS/MS works by sending the peptides through a RP-HPLC column which separates the peptides based on their hydrophobicity. Then, the peptides are analyzed by

a mass analyzer one at a time based on their mass then the mass to charge ratio is determined for the peptide as a whole. Next, the peptides are analyzed by another mass analyzer and a mass to charge ratio is determined for the peptide as a whole then another mass to charge ratio is determined for the peptide with one or more amino acids cleaved at the amide bond by kinetic energy. The difference between the whole peptide and the peptide minus one amino acid corresponds to the mass to charge ratio for that amino acid. This continues for several cycles. Then, the computer searches for a known peptide sequence that uniquely corresponds to the mass to charge ratio for that peptide.

Four samples were sent to the University of Washington in St. Louis, MO for LC/MS/MS analysis. The column that was utilized was a proteomic column with a 75 u diameter. It was 10 cm in length and packed with WATERS Delta-Pak C18, 5 u particle, and a 300 Å pore size. The samples were run by Dr. Ilan Vidavsky (Figures 3.12-3.13).

Chapter 3 – Results

3.1 DGD Purification

a. Cell Growth

DGD was purified from plasmid pJKDGD-A2.2 which consists of the DGD gene in *E. coli*. The purification process produced 23.5 g of cells in a white cell pellet grown to a final OD 600 of 0.86.

b. Protein Assay

After each sonication period, the protein concentration of the supernatant was determined via the Bradford method. After the sonicated cells were centrifuged, the dye binding assay showed the protein concentration to be 7.5 mg/mL.

c. Ammonium Sulfate Precipitation and Dialysis

The supernatant of the sonication was then mixed with 3.8 M ammonium sulfate. After centrifugation, a soft white pellet was present, and upon resuspension of the pellet the solution turned pale yellow. The protein concentration of the dissolved pellet was found to be 5.3 mg/mL (Table3.1).

Table 3.1 – UV spectrophotometer results of the purification of DGD showing the protein concentration after sonication and dialysis.

Sample	Volume Used (μL)	Protein Concentration (mg/mL)	Total Volume (mL)
Sonication 2nd period	**5**	**4.0**	**150**
Sonication 3rd period	**5**	**5.3**	**150**
Sonication 4th period	**5**	**6.6**	**150**
Sonication 5th period	**5**	**8.7**	**150**
Sonication 6th period	**5**	**8.7**	**150**
Sonication supernatant	**4**	**7.5**	**150**
Pellet in dialysis buffer	**4**	**5.3**	**100**

d. Ion-Exchange Chromatography

After purification by ion-exchange chromatography, each 4 mL fraction was analyzed for protein concentration through utilization of the Bradford method (see section 2.1.d for column chromatography method). The highest amount of protein was found in column fractions 69-71 (Figure 3.1a). Then, these column fractions were analyzed by SDS-PAGE for purity as described in section 2.1.d (Figure 3.1b). Since, column fractions 69-71 had the highest amount of pure protein they were combined for further experimentation.

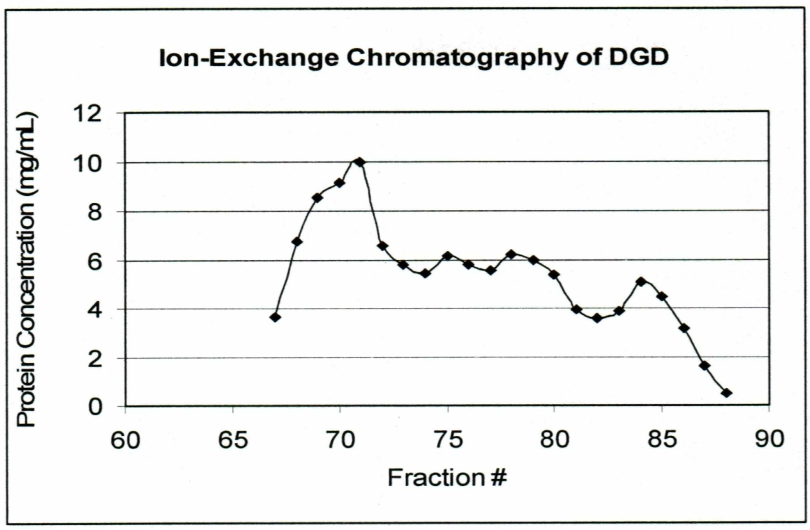

Figure 3.1a - Graph of ion-exchange chromatography data which shows that the highest amount of protein is in fractions 69-71.

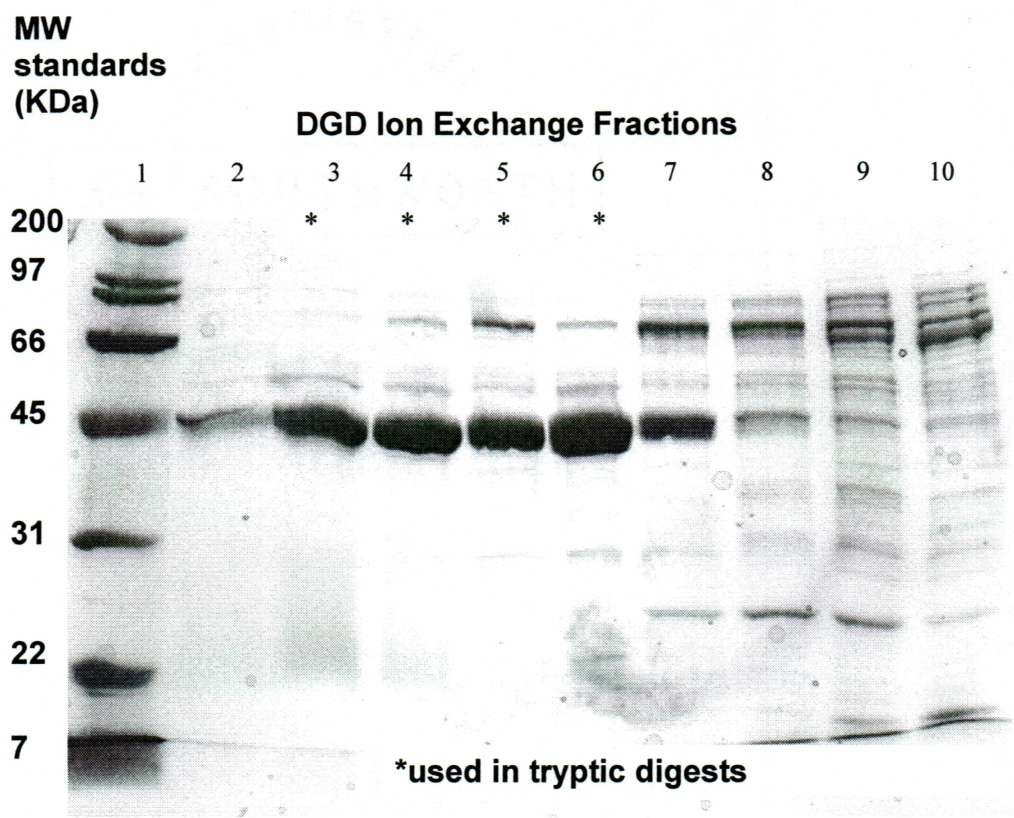

Figure 3.1b - SDS-PAGE which shows that fractions 69-71 contain the purest DGD.

e. Activating Column

Prior to the concentration of the combined column fractions, scans of DGD with and without 2-methylalanine were taken. After the addition of the substrate, the peak at approximately 410 nm, characteristic of PLP, disappeared and a peak at 320 nm, characteristic of PMP, arose. The scan is shown in figure 3.2.

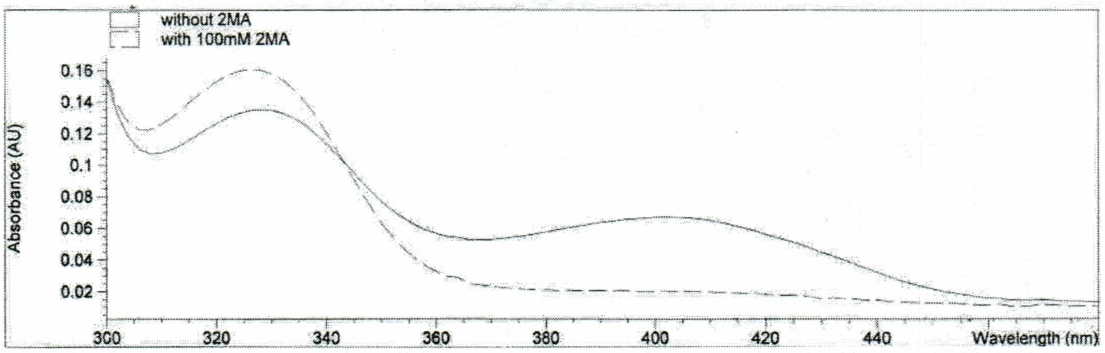

Figure 3.2 – Spectrum scans of DGD without and with 2-methylalanine showing the loss of PLP and the production of PMP after the addition of 2-methylalanine.

In addition to the column purification, an activating column was run to load the DGD with the cofactor, PLP. Fractions 18-23 contained the highest amount of protein, thus these fractions were combined and concentrated to 14 mg/mL with a total volume of 6 mL. The UV spectra results are summarized in table 3.2.

Table 3.2 – UV spectrophotometer results of the purification of DGD showing the protein concentration after ion-exchange chromatography.

Sample	Volume Used (µL)	Protein Concentration (mg/mL)	Total Volume (mL)
Fractions 18-23	**4**	**5.5**	**18**
Concentrated	**2**	**14.0**	**6**

After fractions 18-23 were combined, a kinetic assay was run on the purified DGD. The DGD was found to be active when analyzed by a kinetic assay (Figure 3.3). The specific activity was calculated to be 0.00098 μmol/m·mg.

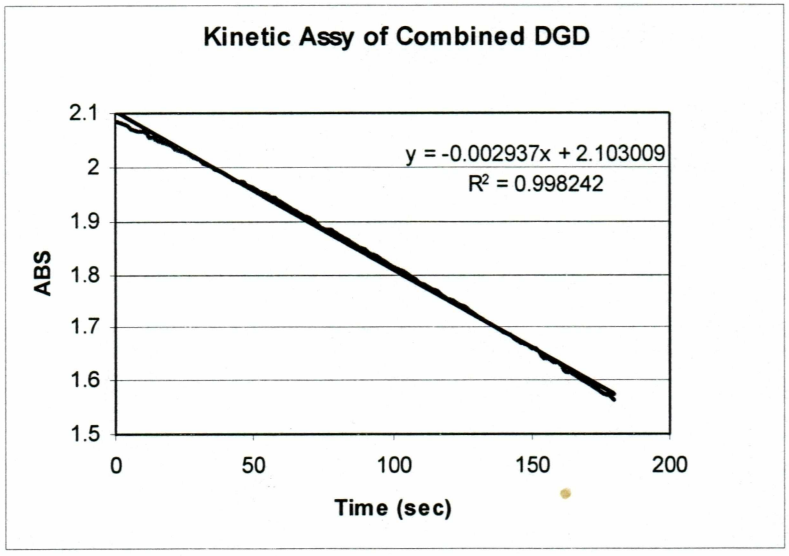

Figure 3.3 – Kinetic assay of combined DGD which shows the loss of pyruvate over time.

3.2 Reduced DGD Purification

A total of 3 mL of protein was collected from the activating column. Utilizing the Bradford method and a BSA standard curve as described in sections 2.1 and 3.1, it was determined that there was 4.3 mg of protein recovered from the column. By using the same technique, it was determined that the second activating column recovered 3.7 mg of reduced protein.

3.3 Digestion Conditions

By digesting DGD with different percentages of trypsin, the optimal percent of DGD to trypsin was found to be 20%. Figure 3.4 shows that DGD is almost completely digested with 20% trypsin. This sample was split into two eppendorf tubes. One was frozen at -70 °C and the other was dried down using a Labconco Centravap system and sent to the University of Washington in St. Louis, MO for LC/MS/MS analysis.

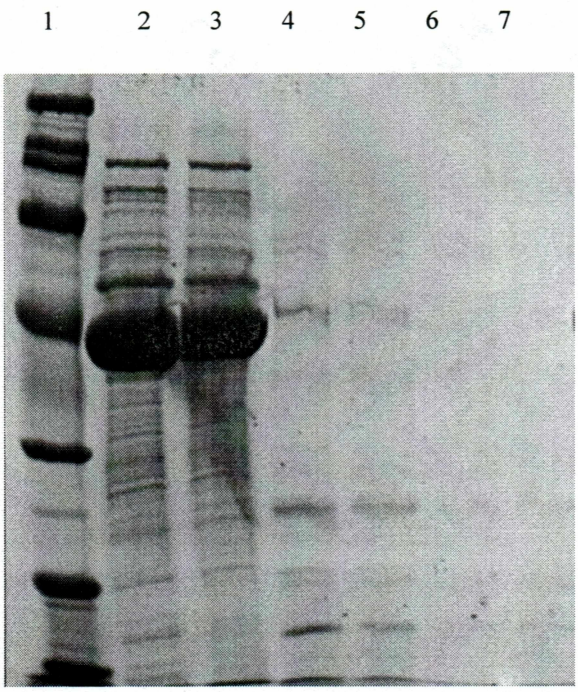

Figure 3.4 – SDS-PAGE gel of digested trypsinized DGD which shows that the enzyme is completely digested by the lack of a band that corresponds to DGD. Lane 1: Molecular weight standard broad range. Lane 2: 33 µg of DGD. Lane 3: 23 µg of DGD without trypsin, shook at 37°C for 21h. Lane 4: 23 µg of DGD with 10% trypsin, shook at 37°C for 21h. Lane 5: 23 µg of DGD with 20% trypsin, shook at 37°C for 21h. Lane 6: 23 µg of DGD with 30% trypsin, shook at 37°C for 21h. Lane 7: 23 µg of DGD with 40% trypsin, shook at 37°C for 21h.

After an optimal percent of trypsin to DGD was determined, the reduced form of DGD was trypsinized in the same fashion with the same amount of trypsin (20%). It was concluded that the digestion reaction was complete enough for use in LC/MS/MS since

most of the band which corresponds to DGD was gone (Figure 3.5). Thus, the reaction was split into two eppendorf tubes. One was frozen at -70 °C and the other was dried down using a Labconco Centravap system and sent to the University of Washington in St. Louis, MO for LC/MS/MS analysis.

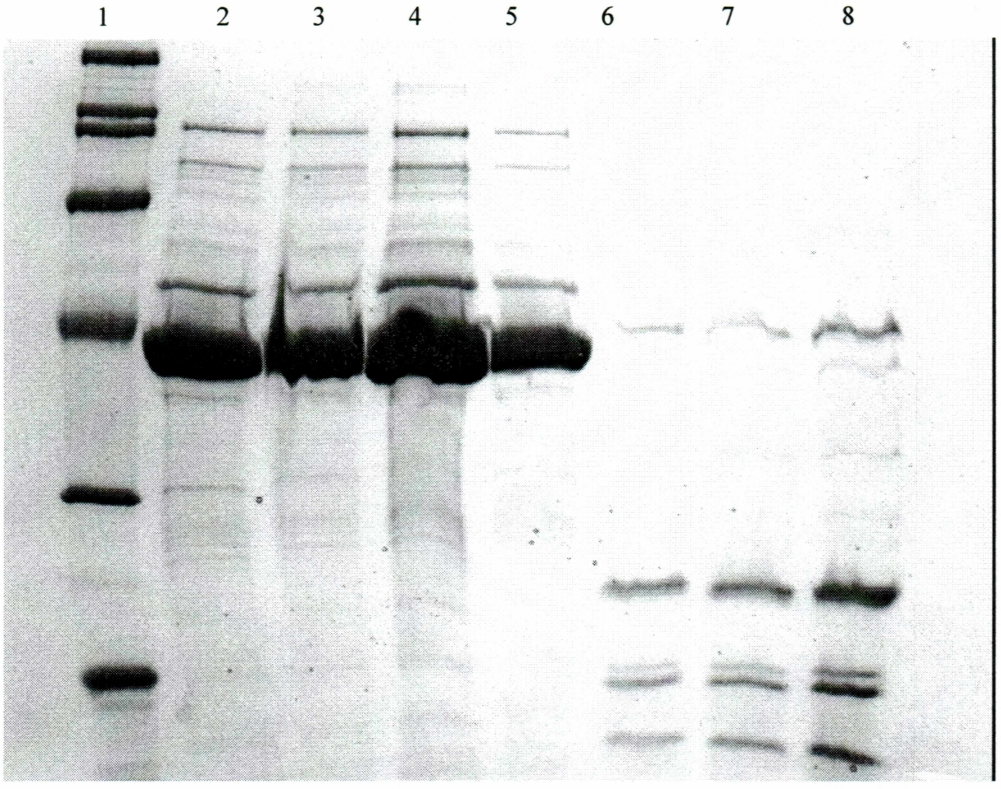

Figure 3.5 – SDS-PAGE gel of digested trypsinized reduced DGD which shows that the reduced enzyme is completely digested by the lack of a band that corresponds to DGD. Lane 1: Molecular weight standard broad range. Lane 2: 4 µg of reduced DGD. Lane 3: 6 µg of reduced DGD. Lane 4: 12 µg of reduced DGD. Lane 5: 1 µg of reduced DGD. Lane 6: 4 µg of reduced DGD with 20% trypsin, shook at 37°C for 21h. Lane 7: 6 µg of reduced DGD with 20% trypsin, shook at 37°C for 21h. Lane 8: 12 µg of reduced DGD with 20% trypsin, shook at 37°C for 21h .

Prior to the digestion of the inhibited enzyme samples, it was imperative to ensure that the enzyme was completely inhibited by the inhibitor. Thus, kinetic assays were

performed at time 0, 2.5, 5 h. The results were imported into MS Excel graphs, and are shown in figures 3.6-3.8.

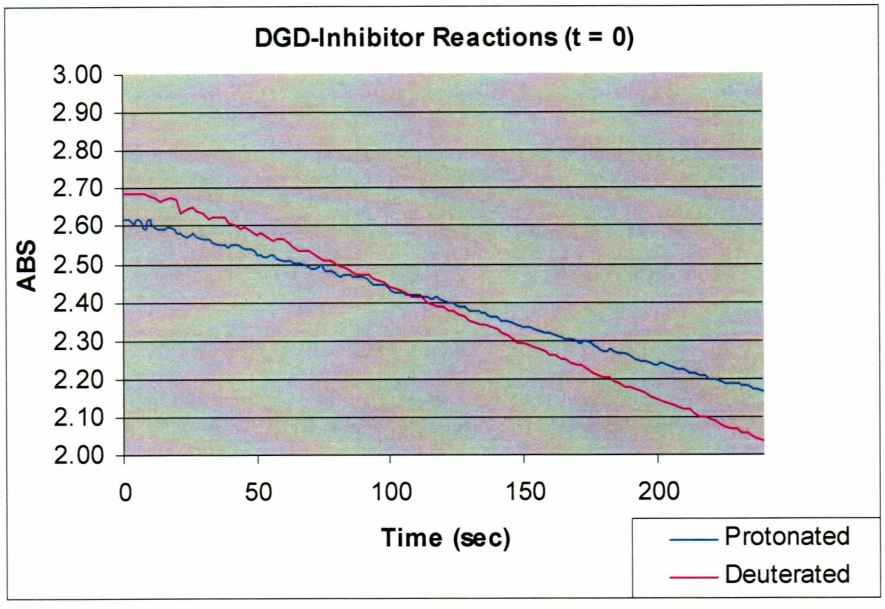

Figure 3.6 – Kinetic assay at the beginning of the inhibition reaction showing a healthy enzyme.

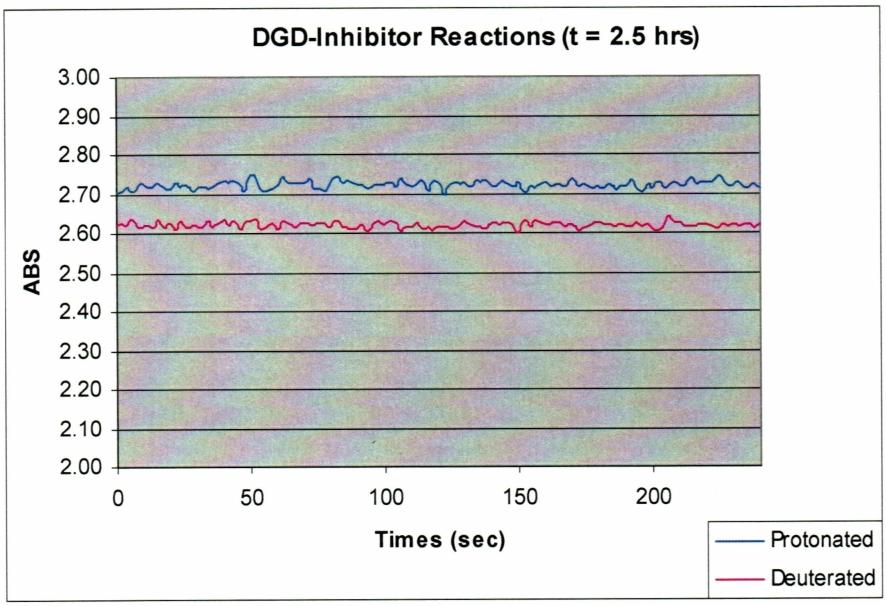

Figure 3.7 – Kinetic assay at time 2.5 h which shows that the enzyme is inactivated.

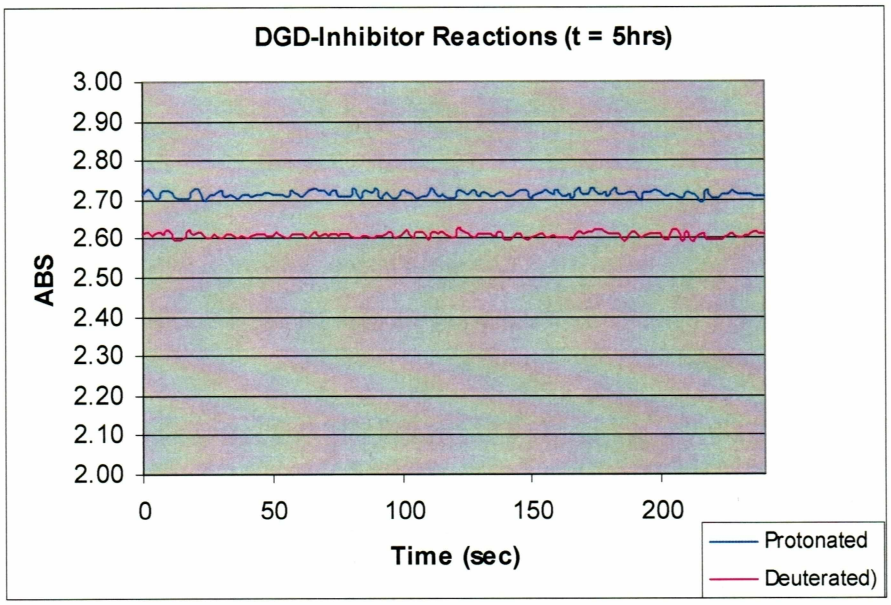

Figure 3.8 – Kinetic assay at time 5 h which shows that the enzyme is completely inactivated.

It was concluded from these graphs, that both the protonated and deuterated inhibitors had completely inhibited the enzyme.

The SDS-PAGE gel of the protonated and deuterated inhibitor reactions is shown in figure 3.9. The reactions were allowed to shake gently for 106 h because the reactions were digested very little at 40 h.

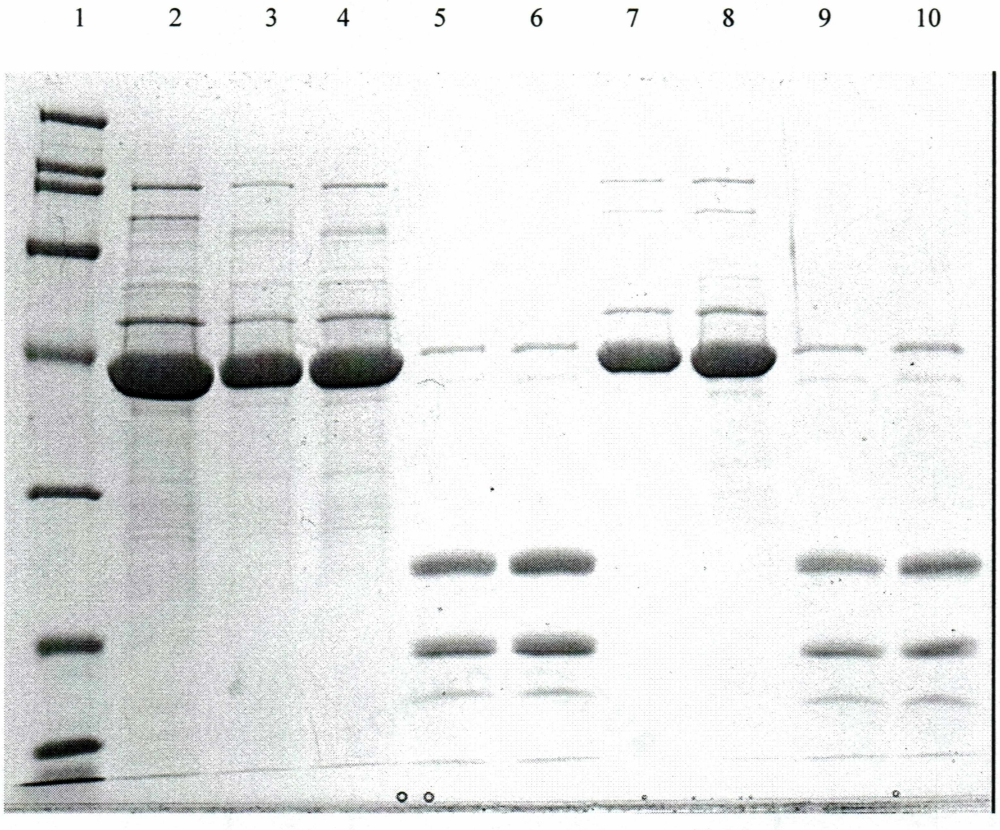

Figure 3.9 – SDS-PAGE gel of digested trypsinized inhibited DGD which shows that the inhibited enzyme is almost completely digested by the reduction of the band that corresponds to DGD. Lane 1: Molecular weight standard broad range. Lane 2: 14 µg of DGD. Lane 3: 7 µg of DGD-F3AIB. Lane 4: 10.5 µg of DGD-F3AIB. Lane 5: 7 µg of DGD-F3AIB, 40% total trypsin shook at 37°C for a total of 106h. Lane 6: 10.5 µg of DGD-F3AIB, 40% total trypsin shook at 37°C for a total of 106h. Lane 7: 7 µg of DGD-F3AIBd_3. Lane 8: 10.5 µg of DGD-F3AIBd_3. Lane 9: 7 µg of DGD-F3AIBd_3, 40% total trypsin shook at 37°C for a total of 106h. Lane 10: 10.5 µg of DGD-F3AIBd_3, 40% total trypsin shook at 37°C for a total of 106h.

3.4 HPLC

Figure 3.10 is a chromatogram of 0.7 µg of DGD digested with trypsin. Four of these peaks were collected and sent for MS analysis with unsuccessful results due to the lack of identification of any peptide (data not shown). There may not have been enough peptide to analyze due to a large amount of the peptide being lost to the column which would explain the lack of results. Figure 3.11 is a comparison of a chromatogram of 0.7 µg of trypsin digested DGD and 0.7 µg of inhibited trypsin digested DGD.

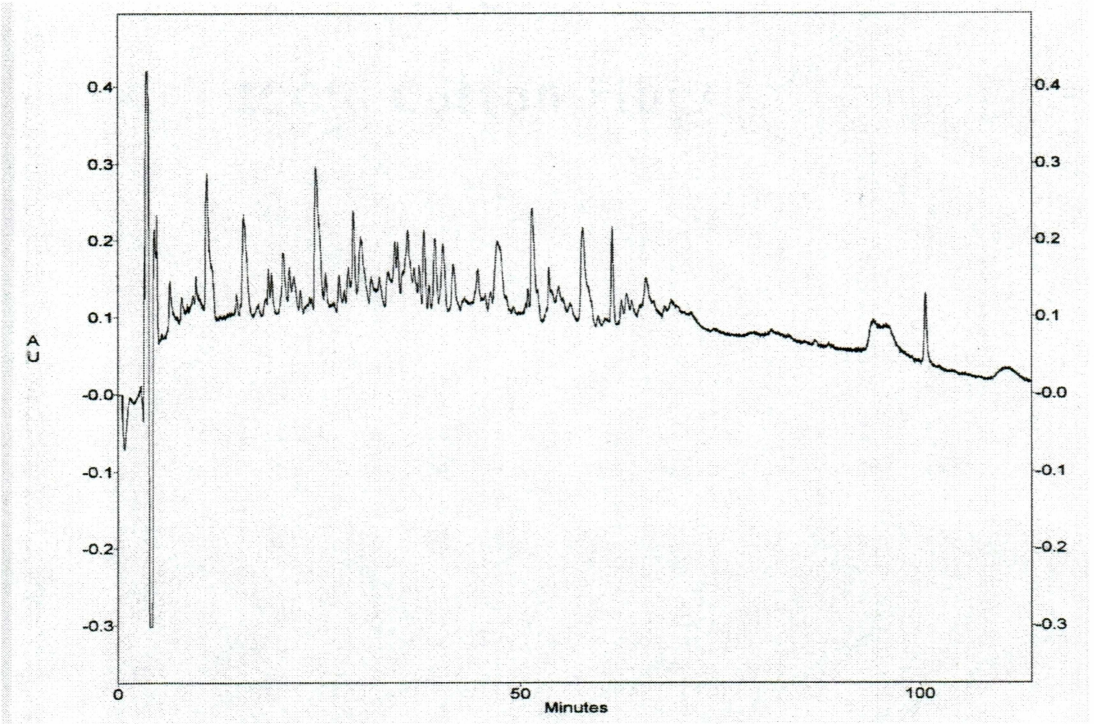

Figure 3.10 – RP-HPLC chromatogram of 0.7 µg of digested DGD where each peak represents a peptide in DGD.

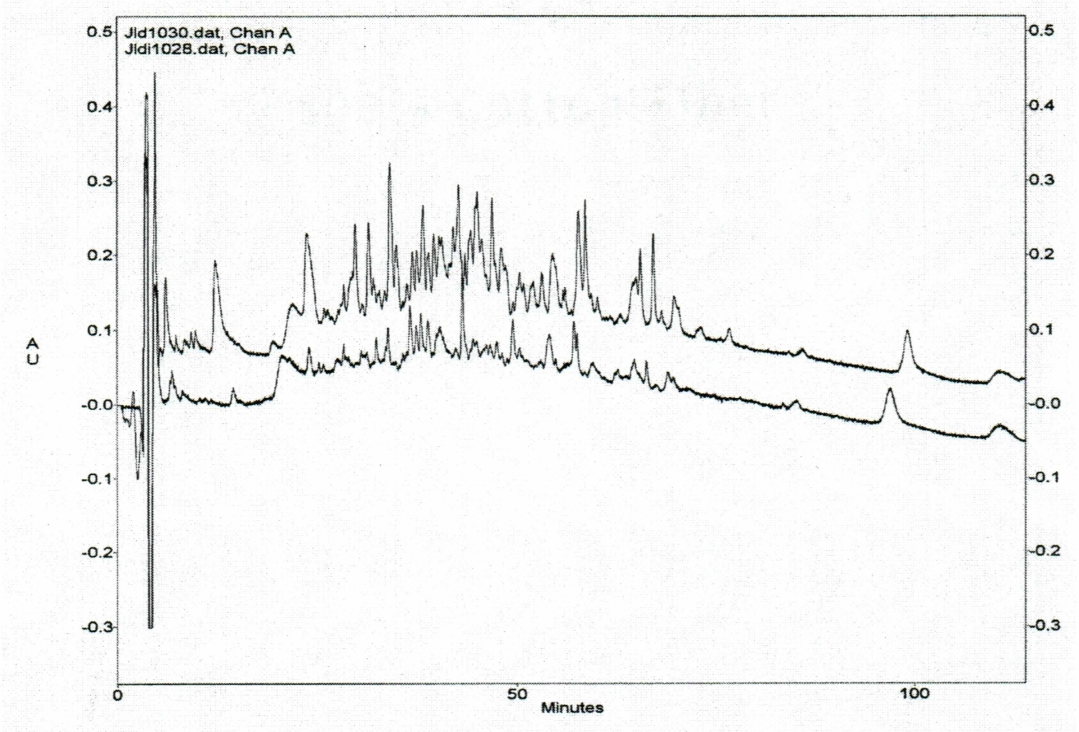

Figure 3.11 - RP-HPLC chromatogram of 0.7 µg of digested DGD (top) and 0.7 µg of inhibited digested DGD (bottom) which shows similarity between the nonmodified and modified DGD.

After MS analysis, it became apparent that collecting peaks from the RP-HPLC was inefficient and non successful. Only one of the four samples sent produced results that remotely resembled a DGD peptide (data not shown). In addition, due to the complexity of the peptide maps it was extremely difficult to try to determine which peaks were the same and which peaks were different when comparing the non inhibited enzyme and the inhibited enzyme to each other. Thus, it was decided to finish the experiments using LC/MS/MS.

3.5 LC/MS/MS

After LC/MS/MS analysis, it was determined that several peptides were found by the instrument that corresponded directly to the known sequence of DGD. Figures 3.12 and 3.13 show the raw data, and table 3.3 indicates which peptides were identified.

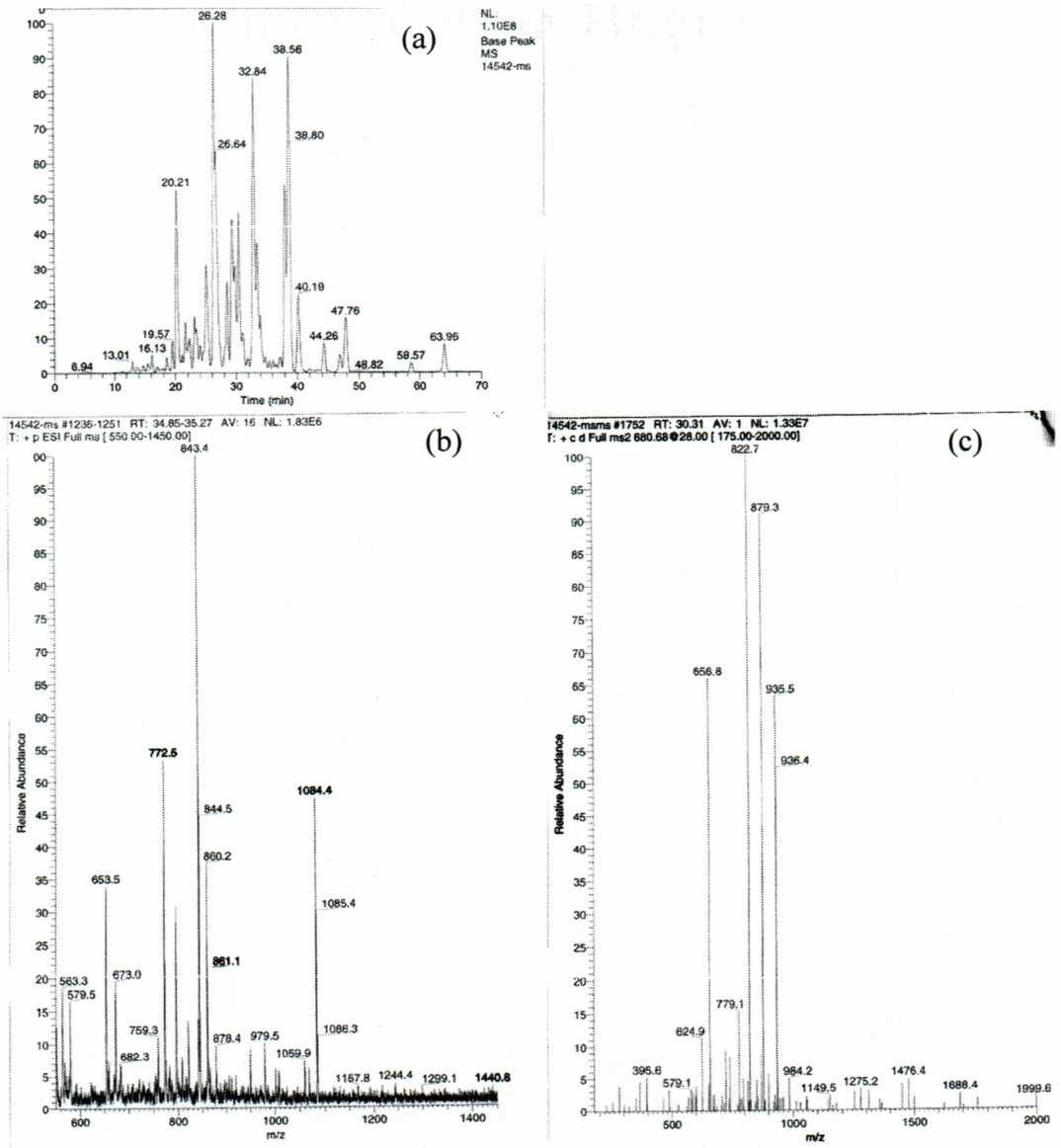

Figure 3.12 – LC/MS/MS of DGD trypsinized with 20% trypsin showing the MS of the digestion mixture and MS/MS of one peptide. (a) total ion current (b) MS of the ions eluting from 34.85 to 35.27 m (c) MS/MS of the peak of m/z 680.68.

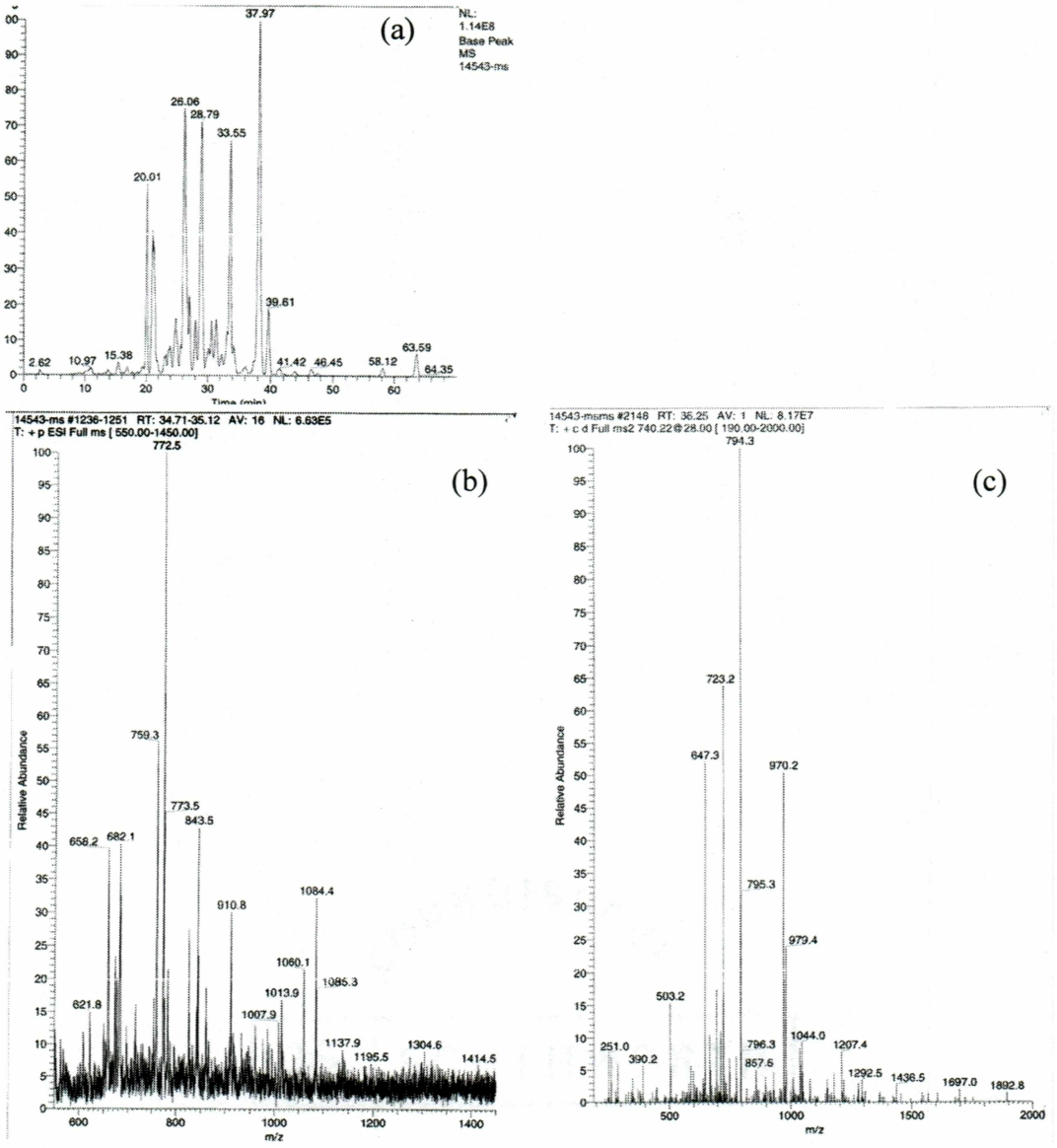

Figure 3.13 – LC/MS/MS of reduced DGD trypsinized with 20% trypsin showing the MS of the digestion mixture and MS/MS of one peptide. (a) total ion current (b) MS of the ions eluting from 34.71 to 35.12 m (c) MS/MS of the peak of m/z 740.2.

Table 3.3 – Peptides of DGD resulting from trypsin cutting at Lys and Arg. (X indicates that the peptide was identified by LC/MS/MS).

Peptide Mass	Position	Peptide Sequence	Found in MS of DGD	Found in MS of Reduced DGD
1355.6	11-Jan	MSLNDDATFWR		
360.2	14-Dec	NAR		
652.39	15-19	QHLVR		
1412.69	20-31	YGGTFEPMIIER	X	
218.15	32-33	AK	X	X
1086.49	34-43	GSFVYDADGR	X	X
3229.6	44-74	AILDFTSGQMSAVLGHCHPE IVSVIGEYAGK		
2127.14	75-93	LDHLFSGMLSRPVVDLATR		X
1166.65	94-104	LANITPPGLDR		
1615.86	105-120	ALLLSTGAESNEAAIR	X	X
349.19	121-123	MAK		
517.33	124-128	LVTGK		
2689.25	129-154	YEIVGFAQSWHGMTGAAASATYSAGR		
2131.14	156-176	GVGPAAVGSFAIPAPFTYRPR		X
451.23	177-179	FER		
2237.04	180-198	NGAYDYLAELDYAFDLIDR		
3233.68	199-230	QSSGNLAAFIAEPILSSGGI IELPDGYMAALK		
478.21	233-236	CEAR		
1572.84	237-251	GMLLILDEAQTGVGR	X	X
1014.45	252-260	TGTMFACQR		
1258.69	261-272	DGVTPDILTLSK	X	X
1953.1	273-292	TLGAGLPLAAIVTSAAIEER		X
2627.36	293-316	AHELGYLFYTTHVSDPLPAA VGLR		X
828.49	317-323	VLDVVQR		X
630.36	324-329	DGLVAR		X
762.36	330-336	ANVMGDR		
288.2	337-338	LR		
946.5	340-347	GLLDLMER		X
924.42	348-355	FDCIGDVR		X
232.14	356-357	GR		
1040.67	358-367	GLLLGVEIVK	X	

Table 3.3 *continued* – Peptides of DGD resulting from trypsin cutting at Lys and Arg. (X indicates that the peptide was identified by LC/MS/MS).

290.15	368-369	DR		
248.16	371-372	TK		
857.44	373-381	EPADGLGAK	X	
389.25	382-384	ITR		
2366.15	385-406	ECMNLGLSMNIVQLPGMGGV FR		
2649.43	407-431	IAPPLTVSEDEIDLGLSLLGQAIER		
203.14	432-433	AL		

Chapter 4 – Discussion

4.1 Purpose of the Project

The question addressed by this project was: "can we use mass spectroscopy to verify the location of the B6 cofactor, pyridoxal 5'-phosphate (PLP) cofactor and the amino acid sequence of the, 2,2-dialkylglycine decarboxylase (DGD)"? The approach used to answer this question was to digest unmodified and modified DGD with trypsin, and then use LC/MS/MS to compare covalently modified (PLP or F3AIB) enzyme with the unmodified enzyme enabling the identification of the peptide of interaction. Because of the significant mass difference between the PLP cofactor and the F3AIB inhibitor, one should be able to use LC/MS/MS to determine whether or not the inhibitor binding site is the same as the PLP binding site.

The reason that DGD was used was because this is a unique enzyme that can both decarboxylate and transaminate amino acid substrates. Also, DGD is a well studied enzyme which is useful because the results of the amino acid content found by LC/MS/MS could be compared back to the known sequence.

4.2 Tryptic Digestions

Many trypsin reactions of DGD and reduced DGD were performed to determine the optimal percent of trypsin and the time required to digest the enzyme. The DGD enzyme was easily digested in 21 h at 37°C as shown by SDS-PAGE. The smallest amount of trypsin required to digest the enzyme was 20%. It was found that urea did not speed up

the digestion reaction. Although 10% trypsin partially digested the enzyme, 20% trypsin provided a more complete digestion. The reduced enzyme was significantly harder to digest. After several attempted digestion reactions were performed on the reduced enzyme; I concluded that there was an impurity in the reaction solution that was inhibiting the cleavage of the enzyme by trypsin. This impurity may be the sodium from the sodium borohydride which changes the confirmation of DGD and results in enzyme inhibition (see section 1.5). The change in confirmation may result in less accessible cleavage sites for trypsin. Thus, the enzyme was concentrated to try to remove the inhibiting impurity along with some of the buffer. A smaller reaction volume was desired so that the collisions between the enzyme and the trypsin would be greater. Concentrating the enzyme did allow the tryptic digest to occur in 21 h similar to the digestion conditions of the non-reduced form of DGD.

The F3AIB-inhibited enzyme from reaction with both protonated and deuterated inhibitor took many more hours to cleave with trypsin than the reduced enzyme. After, a 40 h reaction with 20% trypsin, the F3AIB-inhibited enzyme complex was not nearly digested enough for analysis as shown by SDS-PAGE. Thus, the reaction was allowed to continue for another 66 h with an additional 20% trypsin. Finally, after the 106 h, the F3AIB-inhibited enzyme complex was almost completely digested. The explanation for the increased time may be that the inhibitor is tightly bound to the active site of the enzyme which stabilizes the structure. In this confirmation the inhibitor blocks the active site, making the interior of the enzyme less accessible to the trypsin. One of the reasons that the structure may be more stable with the inhibitor in the active site is due to tighter

interactions between the two monomers. Since the active sites share residues from both monomers, the addition of the inhibitor may provide further cross links between the monomers. This would form a very tight interaction between the two monomers which would greatly inhibit proteolytic action.

4.3 HPLC

After much work with the HPLC, it became apparent that LC/MS/MS could produce better, more efficient results. In my hands, the C18 column from Alltech did not resolve the peaks from the tryptic digestion of DGD well enough to collect and analyze the peaks with good results. The peaks that did come off of the column were very close together which made it very difficult to collect one peak at a time. This resulted in impure collections. This problem became apparent after sending four HPLC collected peaks out for MS analysis. Of these, only one of them produced an amino acid sequence that matched the known peptides in DGD. Thus, it became clear that LC/MS/MS would result in better data.

Although the HPLC results did not provide an answer to the main question, the chromatograms were reproducible and useful in making it clear that the DGD and the F3AIB-DGD complex did not have the same chromatograms after tryptic digestion. These results indicated that the F3AIB was changing the enzyme and that the change was not reversible even after the modified enzyme was cleaved into peptides. This is a strong indication that the inactivation reaction is a covalent attachment of the inhibitor.

4.4 LC/MS/MS

LC/MS/MS is a very useful technique for identifying peptides in a mixture of protein enzymatic digests. The LC/MS/MS instrument can measure the mass of a peptide to the nearest milliamu. If the mass differs by more than one mass unit, it probably does not correspond to the predicted peptide. This is important when a protein containing a lot of peptides is being analyzed. If several of the masses of the peptides are close, mass spectroscopy can distinguish between them. This concept is crucial to the LC/MS/MS results reported here.

LC/MS/MS works by injecting a tryptic digest of a protein onto a small C18 column which separates the peptides with high resolution. Then, the column eluate is sprayed into the source of the mass analyzer, where each droplet of solvent is evaporated off of the peptide. Finally, each peptide is accelerated through the magnetic field to measure its mass. If the peptide is abundant, it is then selected, fragmented by collision with inert gas atoms, and analyzed for the masses of the constituent peptide fragments, hence the term MS/MS. This results in an accurate sequence for each peptide. After the sequence is known, the "Mascot" software is used to identify known proteins that have that particular peptide. If the sequence of the protein is already known, the experimental results can then be compared to the theoretical results. If the peptide is not abundant, the spectrometer does not further analyze it. The "Mascot" software will try to match that mass to any peptide that has that mass. Thus, the user would have to determine what that mass corresponds to.

Based on the sequence of DGD, cleavage of DGD with trypsin should result in 43

peptides (Table 3.3). Upon LC/MS/MS analysis of the trypsinized DGD, only eight of these peptides where identified (Table 3.3). One peptide was identified as DGVTPDILTLSK which corresponds to an active site peptide that contains lysine 272. This is the lysine that has been identified as having PLP bound to it upon reduction.(*3*) Thirteen peptides were identified by the LC/MS/MS analysis of the trypsinized reduced DGD (Table 3.3). There were more peptides identified in the reduced concentrated sample probably because the reduction reaction makes the enzyme looser and more accessible to trypsin.

Upon analysis of the peptides that were in low abundance, a peptide with m/z equal to 1491.64 amu was identified. This is the mass that would be expected if PLP was bound to a tryptic peptide containing lysine 272, i.e. DGVTPDILTLSK. This peptide has a mass of 1258.69 amu, and the mass of a bound PLP was found by Chen and Frey to be 231.14 amu(*25*). Since the C-N bond is reduced, 2 amu would be added resulting in a mass of 1491.83. This mass was not found in the nonreduced sample. The reason that this adduct was found in low abundance is because the reduction of DGD was not performed at an optimal pH. Sodium borohydride is stable in basic conditions; however, in this case sodium borohydride was added to a mixture at pH 7. Consequently, a large portion of sodium borohydride most likely decomposed prior to reducing the PLP-peptide bond. The observation of an excessive amount of bubbles, hydrogen release, supports this conclusion. This would lead to the presence of the peptide containing lysine 272 with and without the bound cofactor, each in low abundance. Also, the decomposition of sodium borohydride could account for the presence of sodium which is an inhibitor of

DGD (Section 1.5). The presence of sodium would change the conformation of the enzyme and reduce the action of trypsin. Hence, the reduced sample would be protected from cleavage by trypsin. Since the peptide containing lysine 272 was found with and without PLP and there was an impurity in the reduced sample that could not be accounted for in the nonreduced sample, I conclude that the reduction reaction was incomplete.

4.5 Future Experiments

In the future, the F3AIB-DGD samples will be analyzed by LC/MS/MS. Because the inhibited enzyme was more difficult to digest, it is likely that there will be fewer peptides identified by LC/MS/MS. One way to avoid this pitfall would be to digest the inhibited samples for a longer period of time using even more trypsin. For this sample, one would look for a mass of 1258.69 amu which corresponds to the peptide containing lysine 272, DGVTPDILTLSK, with the addition of the mass of the inhibitor, the mass of the peptide immediately following lysine 272, and possibly the mass of PLP. The reason that one would look for the mass of the peptide immediately following lysine 272, TLGAGLPLAAIVTSAAIEER (mass=1953.10), in addition to the mass of the peptide containing lysine 272 is because if lysine 272 were bound to the inhibitor, trypsin would no longer recognize it as a cut site. Since it is not known if PLP stays bound to the lysine upon reaction with the inhibitor, one would look for the mass of the two peptides bound together with the inhibitor with and without the mass of PLP. The resulting mass would reveal the chemistry behind this reaction.

References

1. Keller, J. W., Baurick, K. B., Rutt, G. C., O'Malley, M. V., Sonafrank, N. L., Reynolds, R. A., Ebbesson, L. O., and Vajdos, F. F. (1990) *J Biol Chem 265*, 5531-5539.
2. Aaslestad, H. G., and Larson, A. D. (1964) *Journal of Bacteriology 88*, 1296-1303.
3. Keller, J. W., and O'Leary, M. H. (1979) *Biochem Biophys Res Commun 90*, 1104-1110.
4. Dempsey, W. B. (1969) *J Bacteriol 97*, 182-185.
5. Dunathan, H. C. (1966) *Proc Natl Acad Sci U S A 55*, 712-716.
6. Bailey, G. B., Chotamangsa, O., and Vuttivej, K. (1970) *Biochemistry 9*, 3243-3248.
7. Silverman, R. B. (2000) *The Organic Chemistry of Enzyme - Catalyzed Reactions*, Academic Press(New York) p. 366.
8. Lamartiniere, C. A., Itoh, H., and Dempsey, W. B. (1971) *Biochemistry 10*, 4783-4788.
9. Sato, S., Honma, M., and Shimomura, T. (1978) *Agric. Biol. Chem. 42*, 2341-2346.
10. Hedrick, J. L., and Smith, A. J. (1968) *Arch Biochem Biophys 126*, 155-164.
11. Toney, M. D., Hohenester, E., Keller, J. W., and Jansonius, J. N. (1995) *J Mol Biol 245*, 151-179.
12. Hohenester, E., Keller, J. W., and Jansonius, J. N. (1994) *Biochemistry 33*, 13561-13570.
13. Toney, M. D., Keller, J. W., Pauptit, R. A., Jaeger, J., Wise, M. K., Sauder, U., and Jansonius, J. N. (1991) *J Mol Biol 222*, 873-875.
14. Simmaco, M., John, R. A., Barra, D., and Bossa, F. (1986) *FEBS Lett 199*, 39-42.
15. Unkeless, J. C., and Goldman, P. (1970) *Mol Pharmacol 6*, 46-53.
16. Sato, S., Honma, M., and Shimomura, T. (1979) *Agric. Biol. Chem. 43*, 1243-1247.
17. Hayashi, H., Tanase, S., and Snell, E. E. (1986) *J Biol Chem 261*, 11003-11009.
18. Reguera, R. M., Fouce, R. B., Cubria, J. C., Bujidos, M. L., and Ordonez, D. (1995) *Life Sci 56*, 223-230.
19. Relimpio, A., Slebe, J. C., and Martinez-Carrion, M. (1975) *Biochem Biophys Res Commun 63*, 625-634.
20. Wang, E. A., Kallen, R., and Walsh, C. (1981) *J Biol Chem 256*, 6917-6926.
21. Kato, Y., Asano, Y., and Cooper, A. J. (1996) *Dev Neurosci 18*, 505-514.
22. Keller, J. W., and Day, C. S. (1984) *Acta Cryst. C40*, 1224-1226.
23. Davis, M. T., Stahl, D. C., Swiderek, K. M., and Lee, T. D. (1994) *METHODS: A Companion to Methods in Enzymology 6*, 304-314.
24. Huang, E. C., and Henion, J. D. (1990) *American Society for Mass Spectrometry 1*, 158-165.

25. Chen, D., and Frey, P. A. (2001) *Biochemistry 40*, 596-602.
26. Li, Y. F., Hess, S., Pannell, L. K., White Tabor, C., and Tabor, H. (2001) *Proc Natl Acad Sci U S A 98*, 10578-10583.
27. Bradford, M. M. (1976) *Anal Biochem 72*, 248-254.